Materials Advances



View Article Online **REVIEW**



Cite this: Mater. Adv., 2024, **5**, 4055

Received 22nd February 2024, Accepted 14th April 2024

DOI: 10.1039/d4ma00182f

rsc.li/materials-advances

Recent advancement in viologen functionalized porous organic polymers (vPOPs) for energy and environmental remediation

Pampa Jhariat b and Tamas Panda **

A rise in the concentration of hazardous and noxious substances in the environment due to industrialization and population expansion has begun to disrupt the ecological equilibrium. It is of utmost importance to monitor and efficiently manage these pollutants through adsorption techniques or catalytic degradation. Viologen-based porous organic polymers (vPOPs) are a class of porous polymeric materials composed of 4.4'-bipyridinium ions along with other small organic molecules linked together by strong covalent bonds. They have garnered attention as a viable platform for many applications, particularly in the realm of effective environmental remediation. This advancement has generated prospects for the development of more advanced techniques for eliminating contaminants, segregating chemicals, converting gases, and transforming energy. The purpose of this study is to provide an overview of the most recent advancements and successes in the production, utilization, and structural engineering of vPOPs and associated composite materials to remediate environmental problems. This detailed study seeks to provide insights into the potential of vPOPs as viable materials for addressing environmental challenges and stimulating additional research in this emerging sector. This paper provides an analysis of the perspectives about the challenges, opportunities, practical applications, and prospects of these materials in advanced remediation technology for the next generation.

Introduction

Environmental remediation is a methodical procedure designed to address pollution- or contamination-related environmental issues. The main goals are to safeguard human health and the ecosystem while returning the impacted region to its pre-pollution condition. The worldwide population had a notable upsurge throughout the twentieth century, resulting in considerable growth in both commercial and agricultural sectors. Significant human endeavours generate enormous quantities of environmentally detrimental garbage from industrial and agricultural sources, 2,3 significantly contributing to many environmental challenges, such as global warming and the contamination of land, air, and water bodies. Furthermore, the rapid depletion of fossil fuel supplies as a result of extensive global energy use has presented enormous obstacles to the progress and long-term viability of the human population.⁴⁻⁷ To accomplish the goals of protecting human health and the ecosystem, it is essential to actively participate in the development and investigation of novel materials that are

specifically designed to meet certain criteria. This is crucial for fostering socioeconomic development and supporting the promotion of ecologically sustainable activities.8

The rise and notable advancement of porous materials in recent years have highlighted the significant influence of porosity in enhancing the outstanding performance of a material across many applications. 9,10 Porous materials are crucial for many developing technologies and applications because of their unique inherent qualities, including an extensive surface area, versatile synthetic capabilities, adaptive structure, and other notable features. 11-13

In recent decades, numerous novel porous materials have emerged and progressed, encompassing microporous, mesoporous, and macroporous structures. These materials consist of porous organic polymers (POPs), covalent-organic frameworks (COFs), and metal-organic frameworks (MOFs). 14-17 Amidst the proliferation of recently developed materials, there has been a renewed scientific interest in POPs owing to their unique capacity to combine the properties of porous and polymeric substances. POPs are metalfree polymeric organic materials that are predominantly composed of complex molecular structures made up of lightweight elements including carbon, hydrogen, oxygen, nitrogen, and boron. 18-20

In general, porous organic polymers (POPs) exhibit numerous structural and physicochemical benefits in comparison to

^a Centre for Clean Environment, Vellore Institute of Technology, Vellore, Tamil Nadu 632014, India. E-mail: tamaskumarpanda@vit.ac.in

^b Department of Chemistry, School of Advanced Sciences, Vellore Institute of Technology, Vellore, Tamil Nadu 632014, India

conventional and modern porous materials.21 These benefits placed them at the vanguard of the forthcoming generation of multipurpose functional materials. POPs offer many advantages compared to traditional inorganic substances such as activated carbons, zeolites, etc. These advantages include a significant surface area, low density, and strong physicochemical durability. In addition, it is possible to incorporate functional components into POP structures via modifications that occur both before and after synthesis. The pre-synthetic methods offer an extensive range of chemical reactions and the adaptability of monomer design affords considerable potential for the modification of functionalities. 22-24 On the other hand, post-synthetic modification functions as a potent mechanism to enhance the porous architecture's functional versatility. Redox switches are the most frequently observed molecular switch types in POPs. 25,26 These switches are susceptible to alteration when the redox potential of their surroundings alters. A variety of applications of redox switches involve the removal of substances from the environment, such as dyes, iodine, and oxoanions. They are also utilized as electrochemical devices, drug delivery systems, actuators, and sensors.27-29 Different forms of 4,4'-bipyridine, often referred to as viologens, are specific types of redox molecular switches that have been the subject of extensive research. Owing to their positive charge, these switches are amenable to reversible reduction via chemical or electrical reduction methods to radical cationic or neutral species (Scheme 1).30-33 The incorporation of viologen moieties into polymeric frameworks to form viologen-based porous organic polymers (vPOPs) presents a multitude of benefits: (i) the radical cationic species remain in an unstable state for prolonged durations under ambient conditions as the extended polymeric structures stabilize the radicals. (ii) In applications that rely on the in situ generation of radical cationic species, polymeric viologens frequently demonstrate enhanced performance in comparison to monomers and dimers, owing to their improved charge transfer capabilities. (iii) The porosity of vPOPs makes them highly suitable for applications requiring significant surface areas, such as gas adsorption and separation, including reaction catalysis. (iv) The inherent cationic property of vPOPs facilitates the dispersion of insoluble substances. (v) The capacity to regulate the redox state of their viologen moieties enables vPOPs to recognize a variety of substances (such as hydrophobic, hydrophilic, anionic, cationic and other substances) selectively. 34-40 In light of the exponential growth of scientific investigation and recognizing the promising possibilities of new materials, we present a

thorough analysis that explores the current state and recent

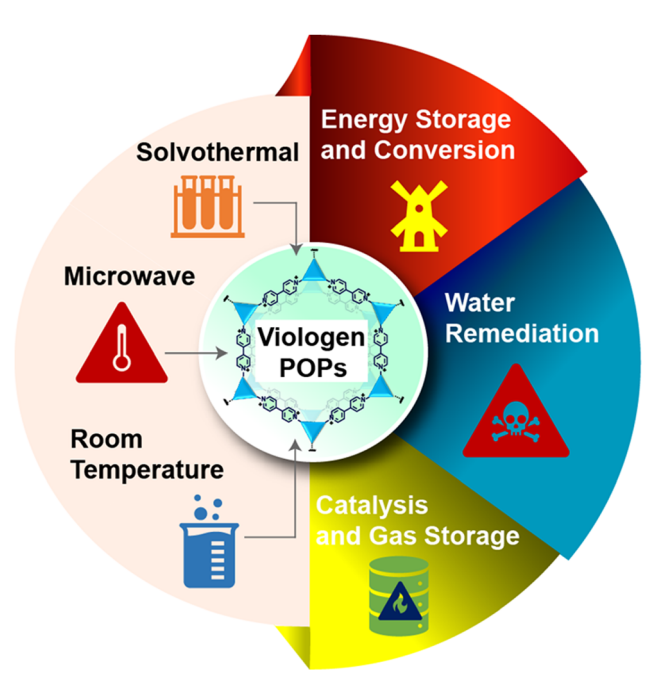


Fig. 1 Representative examples of synthetic methods of vPOPs (right side) including solvothermal, microwave and room temperature synthesis approaches. The left side of the figure represents the application of vPOPs towards energy storage and conversion, water remediation, gas storage and separation, etc.

advancements in various categories of vPOPs used in the diverse environmental context. Their diverse functionalization techniques and synthetic strategies are given particular emphasis. As illustrated in Fig. 1, the review subsequently undertakes a comprehensive analysis of the pragmatic implementations of vPOPs in environmental remediation endeavours, including the storage/segregation of hazardous vapors, elimination of organic/inorganic contaminants, iodine adsorption, and energy storage/conversion. Especially, we shed light on the present obstacles, along with possible advantages, and prospects of these promising materials for energy and environmental remediation. To the best of our knowledge, this review is unique in terms of the application of ionic vPOPs for energy and environmental remediation.

Synthetic methods of vPOPs

As previously mentioned, vPOPs are composed of viologen units, specifically 4,4'-bipyridinium salts, covalently bonded with other organic building blocks. The fabrication of such



Scheme 1 Schematic representation of different redox states of a viologen moiety. The viologen moiety undergoes two reversible reduction reactions. The dicationic state of the viologen moiety is the most stable state of viologen. [R = alkyl/aromatic].

Materials Advances Review

covalent connections, that link 4,4'-bipyridinium ions with organic linkers to build vPOPs, involves several methodical synthetic approaches which are further classified and outlined below. Comprehensive discussions on these synthetic techniques are presented subsequently.

Microwave synthesis

Microwave irradiation presents a viable substitute for traditional techniques utilized in the provision of energy or heat to a given system. This approach functions by using the ability of mobile electric charges in liquids or conducting ions in solids to transform electromagnetic energy into heat. Microwave radiation, consisting of electromagnetic pulses, occupies a position in the electromagnetic spectrum between infrared radiation and radio waves. The frequency spectrum of microwaves spans from 0.3 to 300 GHz, with wavelengths varying from 1 mm to 1 m. A multitude of applications, including microwave radar devices and telecommunications, employ distinct frequencies from this spectrum. By capitalizing on the ability of particular liquids and solids to transform electromagnetic radiation into thermal energy, this method enables chemical reactions to proceed more efficiently. This technological methodology grants synthetic chemists the ability to investigate novel reactions that are unfeasible through the use of conventional thermal techniques. 41,42 In the year 2017,

Trabolsi et al. reported⁴³ for the first time the synthesis of a viologen-based covalent organic gel framework (COGF) through the microwave-assisted Zincke reaction. A triamine-based reactant [1,3,5-tris(4-aminophenyl)benzene] was combined with a Zincke salt (1,1-bis(2,4-dinitrophenyl)-[4,4'-bipyridine]-1,1diium dichloride) in an EtOH-water (4:1) solvent mixture and the resulting mixture was then subjected to 2.45 GHz microwave irradiation for one hour at 100 °C in a 100 mL microwave reaction vessel. The outcome of this procedure was a sheet-like viscoelastic/gel organic framework (COGF). Following the completion of these reactions, the synthesized COGF was utilized to extract iodine in the cyclohexane phase in an efficient manner, as discussed later in the section I₂ uptake. Furthermore, the aforementioned research group utilized microwave irradiation to incorporate azacalix[4]arene, an organic macrocycle, into the structure of a viologen-based covalent organic framework (ACA-COF).44 The ACA-COF has been utilized in the adsorption of uric acid and creatinine, which are critical byproducts produced during hemodialysis in patients suffering from renal failure. The detailed reports of other microwave-synthesized vPOPs are presented in Table 1.

Solvothermal synthesis

Solvothermal synthesis is a well-known technique for synthesizing vPOPs, which has resulted in the development of a wide

Table 1 Tabular representation of synthesis methods of vPOPs

T1.2 COP, ** Microwave Menshutkin reaction MeCN, 89 °C, 1 h	S. no.	vPOPs	Methods for synthesis of vPOPs	Name reactions for the synthesis of vPOPs	Reaction conditions	Ref.
T1.2	T1.1	COGF	Microwave	Zincke reaction	EtOH: H ₂ O (1:1), 100 °C, 2 h	43
T1.4 TFAM-BDNP Microwave Zincke reaction EtOH: H ₂ O (1:1), 100 °C, 2 h 67 T1.5 PV-COF Microwave Zincke reaction EtOH: H ₂ O (1:1), 120 °C, 72 h 82 T1.6 CONs Solvothermal Zincke reaction EtOH: H ₂ O (1:1), 120 °C, 72 h 89 T1.7 COTS Solvothermal Zincke reaction McCN: H ₂ O (1:1), 120 °C, 72 h 45 T1.9 HS Solvothermal Zincke reaction EtOH: H ₂ O (4:1), 120 °C, 72 h 45 T1.10 HT Solvothermal Zincke reaction EtOH: H ₂ O (4:1), 120 °C, 72 h 45 T1.11 Compound-1 Solvothermal Zincke reaction EtOH: H ₂ O (4:1), 120 °C, 72 h 46 T1.12 V-PCIF-X Solvothermal Zincke reaction DMF, 180 °C, 48 h 78 T1.14 TZ-PAF Solvothermal Zincke reaction McOH: EtOH: H ₂ O (1:1), 120 °C, 72 h 66 T1.15 PC-COF Solvothermal Zincke reaction EtOH: H ₂ O (1:1), 120 °C, 72 h 66 T1.16 VGC Solvothermal	T1.2	COP_1^{++}	Microwave	Menshutkin reaction		59
T1.4 TFAM-BDNP Microwave Zincke reaction EtOH: H ₂ O (1:1), 100 °C, 2 h 67 T1.5 PV-COF Microwave Zincke reaction EtOH: H ₂ O (1:1), 120 °C, 72 h 82 T1.6 CONs Solvothermal Zincke reaction EtOH: H ₂ O (1:1), 120 °C, 72 h 89 T1.7 COTS Solvothermal Zincke reaction McCN: H ₂ O (1:1), 120 °C, 72 h 45 T1.9 HS Solvothermal Zincke reaction EtOH: H ₂ O (4:1), 120 °C, 72 h 45 T1.10 HT Solvothermal Zincke reaction EtOH: H ₂ O (4:1), 120 °C, 72 h 45 T1.11 Compound-1 Solvothermal Zincke reaction EtOH: H ₂ O (4:1), 120 °C, 72 h 46 T1.12 V-PCIF-X Solvothermal Zincke reaction DMF, 180 °C, 48 h 78 T1.14 TZ-PAF Solvothermal Zincke reaction McOH: EtOH: H ₂ O (1:1), 120 °C, 72 h 66 T1.15 PC-COF Solvothermal Zincke reaction EtOH: H ₂ O (1:1), 120 °C, 72 h 66 T1.16 VGC Solvothermal	T1.3	ACA-COF	Microwave	Zincke reaction	EtOH: H ₂ O (1:1), 100 °C, 2 h	44
T1.6 CONS Solvothermal Zincke reaction EtOH: H ₂ O (1: 1), 120 °C, 72 h 89 T1.7 COTS Solvothermal Zincke reaction EtOH: H ₂ O (1: 1), 120 °C, 72 h 89 T1.8 CTN: CI Solvothermal Zincke reaction EtOH: H ₂ O (1: 1), 120 °C, 72 h 45 T1.9 HS Solvothermal Zincke reaction EtOH: H ₂ O (4: 1), 120 °C, 72 h 43 T1.10 HT Solvothermal Zincke reaction EtOH: H ₂ O (4: 1), 120 °C, 72 h 43 T1.11 Compound-1 Solvothermal Zincke reaction 1,4-Dioxane: EtOH: chlorobenzene 46 T1.12 V-PCIF-X Solvothermal Zincke reaction DMF, 180 °C, 72 h 78 T1.13 VBCOP Solvothermal Zincke reaction MeOH: dioxane (1: 1), 120 °C, 72 h 65 T1.14 TZ-PAF Solvothermal Zincke reaction THF: H ₂ O (1: 1), 100 °C, 72 h 66 T1.15 PC-COF Solvothermal Zincke reaction AcOH: EtOH: H ₂ O, (1: 1), 100 °C, 72 h 80 T1.16 VGC Solvothermal Zincke reaction EtOH: H ₂ O (4: 1), 120 °C, 72 h 80 T1.18 VMEL Solvothermal Zincke reaction EtOH: H ₂ O (4: 1), 120 °C, 72 h 80 T1.18 VMEL Solvothermal Zincke reaction EtOH: H ₂ O (4: 1), 120 °C, 72 h 80 T1.19 VBPDP Solvothermal Zincke reaction EtOH: H ₂ O (4: 1), 120 °C, 72 h 81 T1.19 VBPDP Solvothermal Zincke reaction EtOH: H ₂ O (4: 1), 120 °C, 72 h 81 T1.21 POF(Co)-Vg-COF Solvothermal Zincke reaction EtOH: H ₂ O (4: 1), 120 °C, 72 h 81 T1.22 IISERP-POF9 Solvothermal Bakelite bond formation Dioxane: THF, 200 °C, 72 h 83 T1.23 IISERP-POF9 Solvothermal Zincke reaction EtOH: H ₂ O (4: 1), 120 °C, 72 h 83 T1.24 IISERP-POF9 Solvothermal Zincke reaction EtOH: H ₂ O (4: 1), 120 °C, 72 h 83 T1.25 SCU-COF-1 Solvothermal Zincke reaction EtOH: H ₂ O (4: 1), 120 °C, 72 h 83 T1.24 IISERP-POF9 Solvothermal Zincke reaction Dioxane: THF, 200 °C, 72 h 83 T1.25 SCU-COF-1 Solvothermal Schiff base reaction Dioxane: THF, 200 °C, 72 h 84 T1.26 BD-POP	T1.4	TFAM-BDNP	Microwave	Zincke reaction	EtOH: H ₂ O (4:1), 100 °C, 2 h	67
T1.7 COTs Solvothermal Zincke reaction EtOH: H ₂ O (1:1), 120 °C, 72 h 89 T1.8 cCTN:Cl ⁻ Solvothermal Zincke reaction McCN: H ₂ O (1:1), 120 °C, 72 h 45 T1.9 HS Solvothermal Zincke reaction EtOH: H ₂ O (4:1), 120 °C, 72 h 45 T1.10 HT Solvothermal Zincke reaction EtOH: H ₂ O (4:1), 120 °C, 72 h 46 T1.11 Compound-1 Solvothermal Zincke reaction DMF, 180 °C, 48 h 78 T1.12 V-PCIF-X Solvothermal Zincke reaction McOH: dioxane (1:1), 120 °C, 72 h 65 T1.13 VBCOP Solvothermal Zincke reaction McOH: BtOH: H ₂ O (1:1), 100 °C, 72 h 65 T1.14 TZ-PAF Solvothermal Zincke reaction THF: H ₂ O (1:1), 100 °C, 72 h 65 T1.15 PC-COF Solvothermal Zincke reaction EtOH: H ₂ O (4:1), 120 °C, 72 h 80 T1.17 vGC Solvothermal Zincke reaction EtOH: H ₂ O (4:1), 120 °C, 72 h 80 T1.17 vGC Solvothermal<	T1.5	PV-COF	Microwave	Zincke reaction	EtOH: H ₂ O (1:1), 100 °C, 2 h	82
T1.8 cCTN:Cl Solvothermal Zincke reaction MeCN:H ₂ O (10:1), 120 °C, 72 h 45 T1.9 HS Solvothermal Zincke reaction EtOH:H ₂ O (4:1), 120 °C, 72 h 43 T1.10 HT Solvothermal Zincke reaction EtOH:H ₂ O (4:1), 120 °C, 72 h T1.11 Compound-1 Solvothermal Zincke reaction 1,4-Dioxane:EtOH:chlorobenzene 46 T1.12 V-PCIF-X Solvothermal Zincke reaction MeOH:dioxane (1:1), 120 °C, 72 h T1.13 VBCOP Solvothermal Zincke reaction MeOH:dioxane (1:1), 120 °C, 72 h 65 T1.14 TZ-PAF Solvothermal Zincke reaction MeOH:EtOH:H ₂ O (1:1), 100 °C, 72 h 66 T1.15 PC-COF Solvothermal Zincke reaction AcOH:EtOH:H ₂ O, 100 °C, 168 h 60 T1.16 vGC Solvothermal Zincke reaction EtOH:H ₂ O (4:1), 120 °C, 72 h 80 T1.17 vGAC Solvothermal Zincke reaction EtOH:H ₂ O (4:1), 120 °C, 72 h 80 T1.19 vBPDP Solvothermal Zincke reaction EtOH:H ₂ O (4:1), 120 °C, 72 h 81 T1.20 VIP-X Solvothermal Zincke reaction EtOH:H ₂ O (4:1), 120 °C, 72 h 81 T1.21 Por(Co)-Vg-COF Solvothermal Zincke reaction EtOH:H ₂ O (4:1), 120 °C, 72 h 81 T1.22 IISERP-POF9 Solvothermal Bakelite bond formation Dioxane:THF, 200 °C, 72 h 83 T1.23 IISERP-POF9 Solvothermal Zincke reaction EtOH:H ₂ O (4:1), 90 °C, 72 h 83 T1.24 IISERP-POF9 Solvothermal Bakelite bond formation Dioxane:THF, 200 °C, 72 h 83 T1.25 AN-POP Solvothermal Zincke reaction EtOH:H ₂ O (4:1), 120 °C, 72 h 83 T1.26 BD-POP Solvothermal Zincke reaction EtOH:H ₂ O (4:1), 120 °C, 72 h 85 T1.27 SCU-COF-1 Solvothermal Zincke reaction EtOH:H ₂ O (4:1), 120 °C, 72 h 85 T1.28 TPVCB[7] Room temperature Schiff base reaction DCM:H ₂ O, 72 h 48 T1.29 V2DP Room temperature Schiff base reaction D-OCB:BuOH (7:3), 24 h 47 T1.30 RT-iCOF Room temperature Schiff base reaction O-DCB:BuOH (7:3), 24 h 87 T1.31 IPOP Solvothermal Menshutkin reaction MeCN, 90 °C, 72 h 102	T1.6	CONs	Solvothermal	Zincke reaction	EtOH: H ₂ O (1:1), 120 °C, 72 h	89
T1.9 HS Solvothermal Zincke reaction EtOH: H ₂ O (4:1), 120 °C, 72 h T1.10 HT Solvothermal Zincke reaction EtOH: H ₂ O (4:1), 120 °C, 72 h T1.11 Compound-1 Solvothermal Zincke reaction 1,4-Dioxane: EtOH: chlorobenzene (1:1:1), 120 °C, 72 h T1.12 V-PCIF-X Solvothermal Zincke reaction DMF, 180 °C, 48 h T1.13 VBCOP Solvothermal Zincke reaction MeOH: dioxane (1:1), 120 °C, 72 h T1.14 TZ-PAF Solvothermal Zincke reaction HFI: H ₂ O (1:1), 100 °C, 72 h T1.15 PC-COF Solvothermal Zincke reaction ACOH: EtOH: H ₂ O, 000 °C, 168 h T1.16 vGC Solvothermal Zincke reaction EtOH: H ₂ O (4:1), 120 °C, 72 h T1.17 vGAC Solvothermal Zincke reaction EtOH: H ₂ O (4:1), 120 °C, 72 h T1.18 vMEL Solvothermal Zincke reaction EtOH: H ₂ O (4:1), 120 °C, 72 h T1.19 vBPDP Solvothermal Zincke reaction EtOH: H ₂ O (4:1), 120 °C, 72 h T1.10 vBPDP Solvothermal Zincke reaction EtOH: H ₂ O (4:1), 120 °C, 72 h T1.21 VP-X Solvothermal Zincke reaction EtOH: H ₂ O (4:1), 120 °C, 72 h T1.22 IISERP-POF9 Solvothermal Bakelite bond formation Dioxane: THF, 200 °C, 72 h T1.23 IISERP-POF9 Solvothermal Bakelite bond formation Dioxane: THF, 200 °C, 72 h T1.24 IISERP-POF9 Solvothermal Zincke reaction EtOH: H ₂ O (4:1), 120 °C, 72 h T1.25 AN-POP Solvothermal Zincke reaction EtOH: H ₂ O (4:1), 120 °C, 72 h T1.26 BD-POP Solvothermal Schiff base reaction EtOH: H ₂ O (4:1), 120 °C, 72 h T1.27 SCU-COF-1 Solvothermal Schiff base reaction DCM: H ₂ O, 72 h T1.28 TpVCB[7] Room temperature Schiff base reaction DCM: H ₂ O, 72 h T1.30 RT-iCOF Room temperature Schiff base reaction O-DCB: BuOH (7:3), 24 h T1.31 IPOP Solvothermal Menshutkin reaction MeCN, 90 °C, 72 h T1.31 IPOP Solvothermal Menshutkin reaction MeCN, 90 °C, 72 h T1.31 IPOP	T1.7	COTs	Solvothermal	Zincke reaction	EtOH: H ₂ O (1:1), 120 °C, 72 h	89
T1.10 HT Solvothermal Zincke reaction	T1.8	$\mathrm{cCTN:Cl}^-$	Solvothermal	Zincke reaction	MeCN: H ₂ O (10:1), 120 °C, 72 h	45
T1.11 Compound-1 Solvothermal Zincke reaction 1,4-Dioxane: EtOH: chlorobenzene 46 (1:1:1), 120 °C, 72 h 78 78 78 78 78 78 78	T1.9	HS	Solvothermal	Zincke reaction	EtOH: H ₂ O (4:1), 120 °C, 72 h	43
T1.12 V-PCIF-X Solvothermal Zincke reaction DMF, 180 °C, 72 h T1.13 VBCOP Solvothermal Zincke reaction MeOH: dioxane (1:1), 120 °C, 72 h T1.14 TZ-PAF Solvothermal Zincke reaction THF: H ₂ O (1:1), 100 °C, 72 h T1.15 PC-COF Solvothermal Zincke reaction AcOH: EtOH: H ₂ O, 100 °C, 168 h T1.16 VGC Solvothermal Zincke reaction EtOH: H ₂ O (4:1), 120 °C, 72 h T1.17 VGAC Solvothermal Zincke reaction EtOH: H ₂ O (4:1), 120 °C, 72 h T1.18 VMEL Solvothermal Zincke reaction EtOH: H ₂ O (4:1), 120 °C, 72 h T1.19 VBPDP Solvothermal Zincke reaction EtOH: H ₂ O (4:1), 120 °C, 72 h T1.19 VIP-X Solvothermal Zincke reaction EtOH: H ₂ O (4:1), 120 °C, 72 h T1.20 VIP-X Solvothermal Zincke reaction EtOH: H ₂ O (4:1), 120 °C, 72 h T1.21 Por(Co)-Vg-COF Solvothermal Zincke reaction EtOH: H ₂ O (4:1), 90 °C, 72 h T1.22 IISERP-POF9 Solvothermal Bakelite bond formation Dioxane: THF, 200 °C, 72 h T1.23 IISERP-POF9 Solvothermal Bakelite bond formation Dioxane: THF, 200 °C, 72 h T1.24 IISERP-POF9 Solvothermal Zincke reaction EtOH: H ₂ O (4:1), 120 °C, 72 h T1.25 AN-POP Solvothermal Zincke reaction EtOH: H ₂ O (4:1), 120 °C, 72 h T1.26 BD-POP Solvothermal Zincke reaction EtOH: H ₂ O (4:1), 120 °C, 72 h T1.27 SCU-COF-1 Solvothermal Schiff base reaction DCM: H ₂ O, 72 h T1.28 TpVCB[7] Room temperature Schiff base reaction TfOH, 144 h T1.29 V2DP Room temperature Schiff base reaction O-DCB: BuOH: acetic acid (19:1:2), 120 °C, 144 h T1.31 IPOP Solvothermal Menshutkin reaction MeCN, 90 °C, 72 h T1.23 IPOP	T1.10	HT	Solvothermal	Zincke reaction	EtOH: $H_2O(4:1)$, 120 °C, 72 h	
T1.12 V-PCIF-X Solvothermal Zincke reaction DMF , $180^{\circ}C$, $48h$ 78 T1.13 VBCOP Solvothermal Zincke reaction DMF , $180^{\circ}C$, $48h$ 65 T1.14 VBCOP Solvothermal Zincke reaction DMF , $180^{\circ}C$, $21h$ 65 T1.14 TZ-PAF Solvothermal Zincke reaction DMF , $180^{\circ}C$, $18h$ 66 T1.15 PC-COF Solvothermal Zincke reaction DMF , $180^{\circ}C$, $110^{\circ}C$, 110	T1.11	Compound-1	Solvothermal	Zincke reaction	1,4-Dioxane : EtOH : chlorobenzene	46
T1.13 VBCOP Solvothermal Zincke reaction MeOH: dioxane $(1:1)$, 120° C, $72h$ 65 T1.14 TZ-PAF Solvothermal Zincke reaction THF: H_2O $(1:1)$, 100° C, $72h$ 66 T1.15 PC-COF Solvothermal Zincke reaction AcOH: EtOH: H_2O , 100° C, $168h$ 60 T1.16 VGC Solvothermal Zincke reaction EtOH: H_2O $(4:1)$, 120° C, $72h$ 80 T1.17 VGAC Solvothermal Zincke reaction EtOH: H_2O $(4:1)$, 120° C, $72h$ 80 T1.18 VMEL Solvothermal Zincke reaction EtOH: H_2O $(4:1)$, 120° C, $72h$ 72 h T1.19 VBPDP Solvothermal Zincke reaction EtOH: H_2O $(4:1)$, 120° C, $72h$ 81 T1.20 VIP-X Solvothermal Menshutkin reaction MeCN, 100° C, 1					(1:1:1), 120 °C, 72 h	
T1.14 TZ-PAF Solvothermal Zincke reaction THF: H_2O (1:1), 100° C, 72 h 66 T1.15 PC-COF Solvothermal Zincke reaction AcOH: EtOH: H_2O , 100° C, 168 h 60 T1.16 vGC Solvothermal Zincke reaction EtOH: H_2O (4:1), 120° C, 72 h 80 T1.17 vGAC Solvothermal Zincke reaction EtOH: H_2O (4:1), 120° C, 72 h 80 T1.18 vMEL Solvothermal Zincke reaction EtOH: H_2O (4:1), 120° C, 72 h 71.19 vBPDP Solvothermal Zincke reaction EtOH: H_2O (4:1), 120° C, 72 h 81 Menshutkin reaction EtOH: H_2O (4:1), 120° C, 72 h 82 T1.20 VIP-X Solvothermal Menshutkin reaction EtOH: H_2O (4:1), 120° C, 72 h 84 T1.21 Por(Co)-Vg-COF Solvothermal Zincke reaction EtOH: H_2O (4:1), 90° C, 90	T1.12	V-PCIF-X	Solvothermal	Zincke reaction	DMF, 180 °C, 48 h	78
T1.15 PC-COF Solvothermal Zincke reaction AcOH:EtOH:H ₂ O, 100 °C, 168 h 60 T1.16 vGC Solvothermal Zincke reaction EtOH:H ₂ O (4:1), 120 °C, 72 h 80 T1.17 vGAC Solvothermal Zincke reaction EtOH:H ₂ O (4:1), 120 °C, 72 h 80 T1.18 vMEL Solvothermal Zincke reaction EtOH:H ₂ O (4:1), 120 °C, 72 h 80 T1.19 vBPDP Solvothermal Zincke reaction EtOH:H ₂ O (4:1), 120 °C, 72 h 81 T1.20 VIP-X Solvothermal Menshutkin reaction EtOH:H ₂ O (4:1), 120 °C, 72 h 81 T1.21 Por(Co)-Vg-COF Solvothermal Zincke reaction EtOH:H ₂ O (4:1), 90 °C, 72 h 81 T1.22 IISERP-POF9 Solvothermal Bakelite bond formation Dioxane:THF, 200 °C, 72 h 83 T1.23 IISERP-POF9 Solvothermal Bakelite bond formation Dioxane: THF, 200 °C, 72 h 83 T1.24 IISERP-POF9 Solvothermal Bakelite bond formation Dioxane:THF, 200 °C, 72 h 83 T1.25 AN-POP Solvothermal Zincke reaction EtOH:H ₂ O (4:1), 120 °C, 72 h 85 T1.26 BD-POP Solvothermal Zincke reaction EtOH:H ₂ O (4:1), 120 °C, 72 h 85 T1.27 SCU-COF-1 Solvothermal Schiff base reaction DCM:H ₂ O, 72 h 86 T1.28 TPVCB[7] Room temperature Schiff base reaction DCM:H ₂ O, 72 h 48 T1.29 V2DP Room temperature Schiff base reaction DCM:H ₂ O, 72 h 48 T1.31 IPOP Solvothermal Menshutkin reaction MeCN, 90 °C, 72 h 102	T1.13	VBCOP	Solvothermal	Zincke reaction	MeOH: dioxane (1:1), 120 °C, 72 h	65
T1.16 vGC Solvothermal Zincke reaction EtOH: H_2O (4:1), $120^{\circ}C$, $72^{\circ}h$ 80 T1.17 vGAC Solvothermal Zincke reaction EtOH: H_2O (4:1), $120^{\circ}C$, $72^{\circ}h$ 71.18 vMEL Solvothermal Zincke reaction EtOH: H_2O (4:1), $120^{\circ}C$, $72^{\circ}h$ 71.19 vBPDP Solvothermal Zincke reaction EtOH: H_2O (4:1), $120^{\circ}C$, $72^{\circ}h$ 71.20 VIP-X Solvothermal Menshutkin reaction MeCN, $100^{\circ}C$, $48^{\circ}h$ 88 T1.21 Por(Co)-Vg-COF Solvothermal Bakelite bond formation Dioxane: THF, $200^{\circ}C$, $72^{\circ}h$ 83 T1.22 IISERP-POF9 Solvothermal Bakelite bond formation Dioxane: THF, $200^{\circ}C$, $72^{\circ}h$ 83 T1.24 IISERP-POF9 Solvothermal Bakelite bond formation Dioxane: THF, $200^{\circ}C$, $72^{\circ}h$ 83 T1.25 AN-POP Solvothermal Bakelite bond formation Dioxane: THF, $200^{\circ}C$, $72^{\circ}h$ 85 T1.26 BD-POP Solvothermal Zincke reaction EtOH: H_2O (4:1), $120^{\circ}C$, $72^{\circ}h$ 85 T1.26 BD-POP Solvothermal Schiff base reaction EtOH: H_2O (4:1), $120^{\circ}C$, $72^{\circ}h$ 85 T1.28 TpVCB[7] Room temperature Schiff base reaction DCM: H_2O , $72^{\circ}h$ 48 T1.29 V2DP Room temperature Schiff base reaction O -DCB: BuOH (7:3), $24^{\circ}h$ 47 T1.30 RT-iCOF Room temperature Schiff base reaction O -DCB: BuOH (7:3), $24^{\circ}h$ 87 T1.31 IPOP Solvothermal Menshutkin reaction MeCN, $90^{\circ}C$, $72^{\circ}h$ 102	T1.14	TZ-PAF	Solvothermal	Zincke reaction	THF: H ₂ O (1:1), 100 °C, 72 h	66
T1.17 vGAC Solvothermal Zincke reaction EtOH:H ₂ O (4:1), 120 °C, 72 h T1.18 vMEL Solvothermal Zincke reaction EtOH:H ₂ O (4:1), 120 °C, 72 h T1.19 vBPDP Solvothermal Zincke reaction EtOH:H ₂ O (4:1), 120 °C, 72 h T1.20 VIP-X Solvothermal Menshutkin reaction MeCN, 100 °C, 48 h T1.21 Por(Co)-Vg-COF Solvothermal Zincke reaction EtOH:H ₂ O (4:1), 90 °C, 72 h T1.22 IISERP-POF9 Solvothermal Bakelite bond formation Dioxane:THF, 200 °C, 72 h T1.23 IISERP-POF9 Solvothermal Bakelite bond formation Dioxane:THF, 200 °C, 72 h T1.24 IISERP-POF9 Solvothermal Bakelite bond formation Dioxane:THF, 200 °C, 72 h T1.25 AN-POP Solvothermal EtOH:H ₂ O (4:1), 120 °C, 72 h T1.26 BD-POP Solvothermal Zincke reaction EtOH:H ₂ O (4:1), 120 °C, 72 h T1.27 SCU-COF-1 Solvothermal Schiff base reaction DCM:H ₂ O (4:1), 120 °C, 72 h T1.28 TpVCB[7] Room temperature Schiff base reaction DCM:H ₂ O, 72 h T1.29 V2DP Room temperature Schiff base reaction TfOH, 144 h T1.30 RT-iCOF Room temperature Schiff base reaction O-DCB:BuOH (7:3), 24 h T1.31 IPOP Solvothermal Menshutkin reaction MeCN, 90 °C, 72 h 102	T1.15	PC-COF	Solvothermal	Zincke reaction	AcOH: EtOH: H ₂ O, 100 °C, 168 h	60
T1.18 vMEL Solvothermal Zincke reaction EtOH: H_2O (4:1), 120 °C, 72 h T1.19 vBPDP Solvothermal Zincke reaction EtOH: H_2O (4:1), 120 °C, 72 h T1.20 VIP-X Solvothermal Menshutkin reaction MeCN, 100 °C, 48 h T1.21 Por(Co)-Vg-COF Solvothermal Zincke reaction EtOH: H_2O (4:1), 90 °C, 72 h T1.22 IISERP-POF9 Solvothermal Bakelite bond formation Dioxane: THF, 200 °C, 72 h T1.23 IISERP-POF9 Solvothermal Bakelite bond formation Dioxane: THF, 200 °C, 72 h T1.24 IISERP-POF9 Solvothermal Bakelite bond formation Dioxane: THF, 200 °C, 72 h T1.25 AN-POP Solvothermal Bakelite bond formation Dioxane: THF, 200 °C, 72 h T1.26 BD-POP Solvothermal Zincke reaction EtOH: H_2O (4:1), 120 °C, 72 h T1.27 SCU-COF-1 Solvothermal Schiff base reaction O -DCB: BuOH: acetic acid (19:1:2), 120 °C, 144 h T1.28 TpVCB[7] Room temperature Schiff base reaction DCM: H_2O , 72 h T1.29 V2DP Room temperature Schiff base reaction O -DCB: BuOH (7:3), 24 h T1.30 RT-iCOF Room temperature Schiff base reaction O -DCB: BuOH (7:3), 24 h T1.31 IPOP Solvothermal Menshutkin reaction MeCN, 90 °C, 72 h	T1.16	vGC	Solvothermal	Zincke reaction	EtOH: H ₂ O (4:1), 120 °C, 72 h	80
T1.19 vBPDP Solvothermal Zincke reaction EtOH: H_2O ($4:1$), 120 °C, 72 h T1.20 VIP-X Solvothermal Menshutkin reaction MeCN, 100 °C, 48 h 88 T1.21 Por(Co)-Vg-COF Solvothermal Zincke reaction EtOH: H_2O ($4:1$), 90 °C, 72 h 84 T1.22 IISERP-POF9 Solvothermal Bakelite bond formation Dioxane: THF, 200 °C, 72 h 83 T1.23 IISERP-POF9 Solvothermal Bakelite bond formation Dioxane: THF, 200 °C, 72 h 83 T1.24 IISERP-POF9 Solvothermal Bakelite bond formation Dioxane: THF, 200 °C, 72 h 83 T1.25 AN-POP Solvothermal Zincke reaction EtOH: H_2O ($4:1$), 120 °C, 72 h 85 T1.26 BD-POP Solvothermal Zincke reaction EtOH: H_2O ($4:1$), 120 °C, 72 h 85 T1.27 SCU-COF-1 Solvothermal Schiff base reaction 0 -DCB: BuOH: acetic acid ($19:1:2$), 120 °C, 144 h 86 T1.28 TpVCB[7] Room temperature Schiff base reaction DCM: H_2O , 72 h 48 T1.29 V2DP Room temperature Schiff base reaction 0 -DCB: BuOH ($7:3$), 24 h 87 T1.31 IPOP Solvothermal Menshutkin reaction MeCN, 90 °C, 72 h 102	T1.17	vGAC	Solvothermal	Zincke reaction	EtOH: H ₂ O (4:1), 120 °C, 72 h	
T1.20 VIP-X Solvothermal Menshutkin reaction MeCN, $100 ^{\circ}\text{C}$, 48h 88 NT.21 Por(Co)-Vg-COF Solvothermal Zincke reaction EtOH: H_2O (4:1), 90 $^{\circ}\text{C}$, 72 h 84 NT.22 IISERP-POF9 Solvothermal Bakelite bond formation Dioxane: THF, 200 $^{\circ}\text{C}$, 72 h 83 T1.23 IISERP-POF9 Solvothermal Bakelite bond formation Dioxane: THF, 200 $^{\circ}\text{C}$, 72 h 83 T1.24 IISERP-POF9 Solvothermal Bakelite bond formation Dioxane: THF, 200 $^{\circ}\text{C}$, 72 h 85 T1.25 AN-POP Solvothermal Zincke reaction EtOH: H_2O (4:1), 120 $^{\circ}\text{C}$, 72 h 85 T1.26 BD-POP Solvothermal Zincke reaction EtOH: H_2O (4:1), 120 $^{\circ}\text{C}$, 72 h 85 T1.27 SCU-COF-1 Solvothermal Schiff base reaction DCM: H_2O (4:1), 120 $^{\circ}\text{C}$, 72 h 48 T1.28 TpVCB[7] Room temperature Schiff base reaction DCM: H_2O , 72 h 48 T1.29 V2DP Room temperature Schiff base reaction TfOH, 144 h 47 T1.30 RT-iCOF Room temperature Schiff base reaction o-DCB: BuOH (7:3), 24 h 87 T1.31 IPOP Solvothermal Menshutkin reaction MeCN, 90 $^{\circ}\text{C}$, 72 h 102	T1.18	vMEL	Solvothermal		EtOH: H ₂ O (4:1), 120 °C, 72 h	
T1.21 Por(Co)-Vg-COF Solvothermal Zincke reaction EtOH: H_2O (4:1), 90 °C, 72 h 84 T1.22 IISERP-POF9 Solvothermal Bakelite bond formation Dioxane: THF, 200 °C, 72 h 83 T1.23 IISERP-POF9 Solvothermal Bakelite bond formation Dioxane: THF, 200 °C, 72 h 83 T1.24 IISERP-POF9 Solvothermal Bakelite bond formation Dioxane: THF, 200 °C, 72 h 85 T1.25 AN-POP Solvothermal Zincke reaction EtOH: H_2O (4:1), 120 °C, 72 h 85 T1.26 BD-POP Solvothermal Zincke reaction EtOH: H_2O (4:1), 120 °C, 72 h 85 T1.27 SCU-COF-1 Solvothermal Schiff base reaction O -DCB: BuOH: acetic acid (19:1:2), 120 °C, 144 h 86 T1.28 TpVCB[7] Room temperature Schiff base reaction O -DCB: BuOH: O -DCB:	T1.19	vBPDP	Solvothermal	Zincke reaction	EtOH: $H_2O(4:1)$, 120 °C, 72 h	
T1.22 IISERP-POF9 Solvothermal Bakelite bond formation Dioxane: THF, 200 °C, 72 h 83 T1.23 IISERP-POF9 Solvothermal Bakelite bond formation Dioxane: THF, 200 °C, 72 h 83 T1.24 IISERP-POF9 Solvothermal Bakelite bond formation Dioxane: THF, 200 °C, 72 h 83 T1.25 AN-POP Solvothermal Zincke reaction EtOH: H ₂ O (4:1), 120 °C, 72 h 85 T1.26 BD-POP Solvothermal Zincke reaction EtOH: H ₂ O (4:1), 120 °C, 72 h 85 T1.27 SCU-COF-1 Solvothermal Schiff base reaction DCM: H ₂ O, 72 h 86 T1.28 TpVCB[7] Room temperature Schiff base reaction DCM: H ₂ O, 72 h 48 T1.29 V2DP Room temperature Schiff base reaction TfOH, 144 h 47 T1.30 RT-iCOF Room temperature Schiff base reaction O-DCB: BuOH (7:3), 24 h 87 T1.31 IPOP Solvothermal Menshutkin reaction MeCN, 90 °C, 72 h 102	T1.20	VIP-X	Solvothermal	Menshutkin reaction	MeCN, 100 °C, 48 h	88
T1.23IISERP-POF9SolvothermalBakelite bond formationDioxane: THF, 200 °C, 72 h83T1.24IISERP-POF9SolvothermalBakelite bond formationDioxane: THF, 200 °C, 72 hT1.25AN-POPSolvothermalZincke reactionEtOH: H_2O (4:1), 120 °C, 72 h85T1.26BD-POPSolvothermalZincke reactionEtOH: H_2O (4:1), 120 °C, 72 h85T1.27SCU-COF-1SolvothermalSchiff base reaction o -DCB: BuOH: acetic acid (19:1:2), 120 °C, 144 h86T1.28TpVCB[7]Room temperatureSchiff base reactionDCM: H_2O , 72 h48T1.29V2DPRoom temperatureSchiff base reaction D -DCB: BuOH (7:3), 24 h47T1.30RT-iCOFRoom temperatureSchiff base reaction o -DCB: BuOH (7:3), 24 h87T1.31IPOPSolvothermalMenshutkin reactionMeCN, 90 °C, 72 h102	T1.21	Por(Co)-Vg-COF	Solvothermal	Zincke reaction	EtOH: H ₂ O (4:1), 90 °C, 72 h	84
T1.24 IISERP-POF9 Solvothermal Bakelite bond formation Dioxane: THF, 200° C, 72° h T1.25 AN-POP Solvothermal Zincke reaction EtOH: H_2O (4:1), 120° C, 72° h 85 T1.26 BD-POP Solvothermal Zincke reaction EtOH: H_2O (4:1), 120° C, 72° h 85 T1.27 SCU-COF-1 Solvothermal Schiff base reaction o -DCB: BuOH: acetic acid (19:1:2), 120° C, 144° h 86 T1.28 TpVCB[7] Room temperature Schiff base reaction DCM: H_2O , 72° h 48 T1.29 V2DP Room temperature Schiff base reaction TfOH, 144° h 47 T1.30 RT-iCOF Room temperature Schiff base reaction o -DCB: BuOH (7:3), 24° h 87 T1.31 IPOP Solvothermal Menshutkin reaction MeCN, 90° C, 72° h 102	T1.22	IISERP-POF9	Solvothermal	Bakelite bond formation	Dioxane: THF, 200 °C, 72 h	83
T1.25 AN-POP Solvothermal Zincke reaction EtOH: H_2O (4:1), $120^{\circ}C$, $72^{\circ}h$ 85 T1.26 BD-POP Solvothermal Zincke reaction EtOH: H_2O (4:1), $120^{\circ}C$, $72^{\circ}h$ 85 T1.27 SCU-COF-1 Solvothermal Schiff base reaction o -DCB: BuOH: acetic acid (19:1:2), $120^{\circ}C$, $144^{\circ}h$ 86 T1.28 TpVCB[7] Room temperature Schiff base reaction DCM: H_2O , $72^{\circ}h$ 48 T1.29 V2DP Room temperature Schiff base reaction TfOH, $144^{\circ}h$ 47 T1.30 RT-iCOF Room temperature Schiff base reaction o -DCB: BuOH (7:3), $24^{\circ}h$ 87 T1.31 IPOP Solvothermal Menshutkin reaction MeCN, $90^{\circ}C$, $72^{\circ}h$ 102	T1.23	IISERP-POF9	Solvothermal	Bakelite bond formation	Dioxane: THF, 200 °C, 72 h	83
T1.26 BD-POP Solvothermal Zincke reaction EtOH: H_2O ($4:1$), 120 °C, 72 h T1.27 SCU-COF-1 Solvothermal Schiff base reaction o -DCB: BuOH: acetic acid ($19:1:2$), 120 °C, 144 h 86 T1.28 TpVCB[7] Room temperature Schiff base reaction DCM: H_2O , 72 h 48 T1.29 V2DP Room temperature Schiff base reaction TfOH, 144 h 47 T1.30 RT-iCOF Room temperature Schiff base reaction o -DCB: BuOH ($7:3$), 24 h 87 T1.31 IPOP Solvothermal Menshutkin reaction MeCN, 90 °C, 72 h 102	T1.24	IISERP-POF9	Solvothermal	Bakelite bond formation	Dioxane: THF, 200 °C, 72 h	
$ \begin{array}{llllllllllllllllllllllllllllllllllll$	T1.25	AN-POP	Solvothermal	Zincke reaction	EtOH: H ₂ O (4:1), 120 °C, 72 h	85
$ \begin{array}{llllllllllllllllllllllllllllllllllll$	T1.26	BD-POP	Solvothermal	Zincke reaction	EtOH: H ₂ O (4:1), 120 °C, 72 h	
T1.29 V2DP Room temperature Schiff base reaction TfOH, 144 h 47 T1.30 RT-iCOF Room temperature Schiff base reaction o-DCB:BuOH (7:3), 24 h 87 T1.31 IPOP Solvothermal Menshutkin reaction MeCN, 90 °C, 72 h 102	T1.27		Solvothermal	Schiff base reaction	o-DCB: BuOH: acetic acid (19:1:2), 120 °C, 144 h	86
T1.30 RT-iCOF Room temperature Schiff base reaction o-DCB: BuOH (7:3), 24 h 87 T1.31 IPOP Solvothermal Menshutkin reaction MeCN, 90 °C, 72 h 102	T1.28	TpVCB[7]			2 /	48
T1.31 IPOP Solvothermal Menshutkin reaction MeCN, 90 °C, 72 h 102	T1.29					
	T1.30					87
T1.32 VCR-POP-1 Solvothermal Knoevenagel condensation DMSO, CS ₂ CO ₃ , 120 °C, 72 h	T1.31				MeCN, 90 °C, 72 h	102
	T1.32	VCR-POP-1	Solvothermal	Knoevenagel condensation	DMSO, CS ₂ CO ₃ , 120 °C, 72 h	110

array of vPOPs utilized in numerous disciplines. This synthetic approach generates vPOPs by combining two or more different monomers or, occasionally, by self-coupling a single monomer. The reaction takes place in a solvent mixture heated to a high temperature, typically (ranging between 90 and 150 °C) for one to three days. Numerous organic monomers are chemically bonded together to form stable covalent bonds under these artificial circumstances. Afterward, these bonds undergo expansion in two or three dimensions, leading to the creation of a kinetically regulated network of vPOPs. Numerous instances of effective vPOP synthesis utilizing the solvothermal technique are examined and listed in Table 1. For example, Wen et al. documented the solvothermal synthesis of a redox-active covalent triazine network based on viologen. The vPOP that was produced was subsequently employed in fuel cell applications as an electrochemical catalyst. 45 Ghosh et al. also described the synthesis of viologen-based vPOPs (compound 1) using a solvothermally aided Zincke reaction. 46 Compound-1 displayed remarkable capacity values for a range of oxoanions, which were comparable to those of several exceptionally efficient compounds documented in the extant literature.

Room temperature synthesis

In this method, the reactants are mixed in a designated solvent or a blend of solvents, often with the inclusion of a catalyst. The mixture is then stirred or kept undisturbed at room temperature for a set period to accomplish the reaction. Using this straightforward synthesis approach, several vPOPs have been synthesized, as mentioned in Table 1. Feng and his group constructed one high-performance electrochemical device with a fully crystalline viologen-based 2D polymer (denoted as V2DP) thin film. 47 The thin film was synthesized through a twodimensional polycondensation approach at room temperature. The resulting V2DP manifests as a self-supporting, crystalline film with a substantial area (exceeding 100 cm²) along with adjustable thickness (ranging from 1 to 65 nm) which was further used in solar cell application, discussed in the section Energy storage and conversion. Trabolsi et al. synthesized a thin film of a polyrotaxanated covalent organic network at room temperature. 48 The film, encapsulated with CB[7], exhibited enhanced mechanical and thermal robustness, along with increased luminescence. Table 1 contains information on additional room-temperature synthesized vPOPs.

The reaction involved in the synthesis of vPOPs

Zincke reaction

The Zincke reaction, a widely recognized name reaction for the synthesis of vPOPs, has been pivotal in the creation of a wide range of vPOPs that are utilized across multiple disciplines. The Zincke reaction converts bipyridine into a quaternary pyridinium salt in two steps. The initial stage involves the S_N2 reaction between 4,4'-bipyridine and 1-chloro-2,4-dinitrobenzene to produce the Zincke salt. A primary amine attacks the most

electrophilic carbon in the Zincke salt and opens the pyridine ring in the second phase. This results in the elimination of 2,4-dinitroaniline, the closing of the ring, and the formation of a quaternized pyridinium ion. It is believed that the ratedetermining step is the opening of the ring, and the reversibility of the reaction produces a crystalline substance and likely permits error correction.³³ In the year 2017, Trabolsi et al. reported⁴³ for the first time the synthesis of crystalline viologen-based covalent organic gel frameworks (COGFs) through the microwave-assisted Zincke reaction and amorphous vPOPs through the solvothermal assisted Zincke reaction (HS and HT). At the same time, Ghosh et al. also described the synthesis of viologen-based vPOPs (compound 1) using the solvothermal-assisted Zincke reaction.⁴⁶ Compound-1 demonstrated extraordinary capture capacity of oxoanions from wastewater. Very recently, our group synthesized a series of vPOPs (vGC, vGAC, vMEL and vBPDP) through the solvothermal assisted Zincke reaction and utilized these vPOPs as metal-free bifunctional electrocatalysts for the oxygen reduction and oxygen evolution reaction which is discussed thoroughly in the Energy storage and conversion section.80 Several vPOPs have been synthesized through the Zincke reaction, as mentioned in Table 1.

Menshutkin reaction

An exhaustively researched $S_{\rm N}2$ reaction, the Menshutkin reaction, is one of the foundational S_N2 reactions in organic and bioorganic chemistry. The reactants are neutral during the reaction, whereas the two products acquire negative and positive charges, respectively. The mechanism underlying the Menshutkin reaction in solution differs significantly from that observed in the gas phase. Specifically, the reaction occurs at a significantly faster rate in a solvent with high polarity compared to that with reduced polarity. In general, polymers comprise a monomer that is modified with an aliphatic alkyl halide, such as chloride. In straightforward S_N2 Menshutkin reactions, halides function well as leaving groups when subjected to nucleophilic attack by the electron-rich nitrogen centres of 4,4'-bipyridine. The crosslinked vPOPs have been synthesized using this methodology.33 There are several vPOPs reported, synthesized through this name reaction and documented in Table 1. For example, Trabolsi et al. reported a vPOP (COP₁⁺⁺) through the microwave-assisted Menshutkin reaction and further employed this vPOP in iodine vapor adsorption.⁴³ Very recently, Moorthy et al. reported a vPOP (IPOP) synthesized through a solvothermal-assisted Menshutkin reaction where they used twisted biaryl as a monomer. They utilized the IPOP as a phase transfer catalyst for the Michal addition reaction (discussed in the Catalysis section).

Schiff-base reaction

Schiff-base condensation is one of the most significant categories of reactions in the synthesis of porous organic polymers. The process, which utilizes amine and aldehyde to functionalize monomers, generates an imine link. For vPOP synthesis, this name reaction is very rarely explored. Very few vPOPs, synthesized through the Schiff base reaction, are reported and

tabulated in Table 1. Feng et al. constructed one highperformance electrochemical device with a fully crystalline viologen-based 2D polymer (denoted as V2DP) thin film through the Schiff base reaction at room temperature. 47 Similarly, Trabolsi et al. synthesized a thin film of a polyrotaxanated covalent organic network through the Schiff base reaction at room temperature.48

Application

Materials Advances

vPOPs for water remediation

One of the extensively explored realms within environmental science focuses on eliminating organic and inorganic pollutants from water. Several methods have been devised to treat polluted wastewater, and among them, the adsorption method stands out as a very promising technology owing to its economical nature, substantial capacity to adsorb pollutants, and ability to selectively remove certain contaminants. Crucial characteristics of adsorbents for pollution removal include high adsorption capacity, rapid kinetics, reusability, and stability. 49,50 The implementation of vPOPs in these kinds of applications provides advantages, notably because of their modifiable charge. Dicationic vPOPs can interact with various anionic poisonous dyes and anions present in polluted water. On the other hand, neutral vPOPs may function as Lewis bases and interact with hydrophobic substances in water.27,51

The increasing demand of a growing human population, coupled with accelerated industrial development and global environmental issues, has profoundly affected the availability of clean water for civilization, leading to serious problems such as water shortages and mounting water pollution. Water pollution has become a major worldwide problem, and the preservation of micro contaminants in water has drawn a significant deal of scientific attention. 52,53 Several sustained enhanced chemical separation technologies have been employed or are being tested to decontaminate clogged water systems, including effluent and salt water, to provide a fresh and pure water supply. Of these, adsorption-based purification technologies have been acknowledged as feasible and eco-friendly alternatives to conventional treatments, which may be attributable to their exceptional efficiency, effortless operation, and costeffectiveness. Significant progress has been made in developing very effective adsorbents for separation methods that rely on sorption in the last several years. 54,55 In the field of pollutant removal from water and wastewater treatment, vPOPs have been regarded as highly promising absorbent substances because of their distinctive properties such as redox activity, tuneable pore diameter, free exchangeable anions and so on. Here, we have categorized pollutants into two classes, namely,: (i) organic pollutants and (ii) inorganic pollutants, and discussed the role of vPOPs in removing them from water thoroughly. Iodine removal from water and iodine capture through vPOPs are also subject to in-depth discussion.

Organic pollutants removal from water. Water bodies worldwide have been shown to contain organic pollutants, including organic colors, pesticides, antibiotics, pharmaceuticals, personal care items, and chemicals produced from oil. This finding has sparked apprehensions over possible adverse effects on both aquatic environments and human well-being. Consequently, there is a growing focus on studying effective methods to remove these pollutants from diverse water sources. In this specific context, research indicates that porous organic polymers based on viologen (vPOPs) demonstrate significant efficacy in efficiently capturing these organic toxins from water solutions.56,57

In a recent exploration, Ghosh et al. delved into the potential of a vPOP (named iVOFm) to effectively eliminate several harmful anionic organic compounds, including pigments, antimicrobial agents, as well as inorganic pollutants (Fig. 2(a)).⁵⁸ The study introduced a solid-state acid vapor-aided approach utilizing silica nanoparticles as templates for designing and synthesizing a macro-micro hierarchical iVOFm. The resulting iVOFm underwent thorough characterization, revealing unique features such as a cationic backbone with densely distributed free counter anions, hierarchical porosity at macro and micro scales, and exceptional chemical stability. Notably, the size and quantity of macropores in iVOFm could be easily adjusted using an appropriate SiO2 nanoparticle template. Here, the customized design of iVOFm employs a synergistic approach, integrating electrostatically induced ion exchange processes, macro-micro pores, and specialized binding sites, to efficiently target and remove the desired contaminants. The efficacy of iVOFm in removing organic dyes, specifically alizarin red S and methyl orange, and antibiotics such as sulfamethazine (SMT) and sulfadimethoxine (SDM) from water was assessed. iVOFm demonstrated swift adsorption capabilities for diverse organic toxins, iodine, and metal-based oxoanions, achieving a clearance efficiency exceeding 93% within 30 s (Fig. 2(b) and (c)). The research further illustrated the successful removal of the antibiotic SDM from water, highlighting a rapid sorption capacity that maintained high effectiveness even in the presence of coexisting anions such as nitrates, chloride, and bromide. The investigation suggested that the exceptional pollutant-trapping efficiency could be attributed to the rapid diffusion of pollutants facilitated by well-structured and interconnected macropores, synergistically interacting with the cationic backbone.

Simultaneously, a comprehensive investigation was carried out to assess how the redox state of the viologen moieties of vPOPs influences the capture of hydrophilic and hydrophobic dyes. Trabolsi et al. synthesized a new type of phosphazene based vPOP (COP₁), for the absorption of neutral fluorescein dye (hydrophilic), cationic rhodamine B dye (hydrophilic), and anionic Nile red dye (hydrophobic) (Fig. 2(d)). The study revealed that both the charge and the level of hydrophilic or hydrophobic nature of both the absorbent and the dye play a crucial role in determining the absorption capacity. Efficient adsorption of fluorescein by the dicationic COP1++ was observed, achieving a remarkable removal rate of 99% in just 4 minutes (Fig. 2(e)).⁵⁹ This high efficiency can be attributed to robust hydrophilic-hydrophilic associations, which are not feasible between fluorescein and radical cationic (COP1+) or neutral

Nile Red

Review

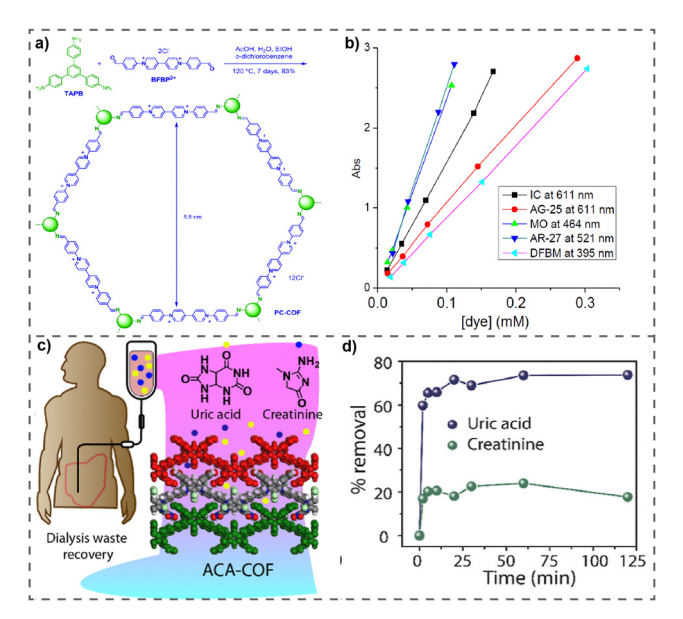
SIO₂ NPs moval efficiencies(%)

Fig. 2 (a) Synthetic route for iVOFm. (b) and (c) Removal kinetics and % removal of all pollutants through iVOFm. Reproduced with permission from ref. 58. Copyright 2022 Wiley-VCH. (d) Schematic representation of the synthesis of COP₁⁺⁺. (e) Bar graphs of adsorption capacities of the cationic, radicalcationic and neutral forms of COP₁ for fluorescein, rhodamine B, and Nile Red. Reproduced with permission from ref. 59. Copyright 2014 the Royal Society of Chemistry.

Pollutants

(COP₁) vPOPs. Similarly, the neutral COP₁ demonstrated significant capability, eliminating approximately 85% of Nile red within an hour. The effectiveness of this removal is likely due to the potential occurrence of hydrophobic interactions between the COP_1^0 and Nile red. Dicationic (COP_1^{++}) and radical cationic (COP₁^{•+}) conjugated organic polymers displayed a maximum removal efficiency of 25% for Nile red. The study's findings suggest that the specificity of vPOPs may be customized for a particular pollutant by altering the redox phase of the viologen moiety. Li et al. explained these anionic dye adsorption phenomena through viologen-based cationic POPs (PC-COF) by the concept of soft and hard acid-base theorem (Fig. 3(a)).60 Anionic dyes are generally considered as soft bases, which will be paired up with viologenbased POPs, and act as soft acids, whereas the Cl⁻ anions are considered as hard bases, paired up with cations from dye considered as hard acids. They synthesized crystalline iminebased vPOPs (PC-COF) and further conducted adsorption studies, examining a range of anionic dyes such as acid green, acid red 27, indigo carmine, methyl orange, and Direct Fast Brown M. Remarkably, this material demonstrated an uptake exceeding 97% for these diverse dyes even at very low concentrations (Fig. 3(b)). The authors attribute the enhanced absorption capacity to the implementation of the hard and soft acid/base approach. In this context, anionic dyes, serving as soft bases, create pairs with the softly acidic vPOPs (PC-COF), while hard Cl ions form pairs with hard Na⁺ ions and these lead to efficient adsorption of toxic dyes. Several vPOPs are reported for this particular removal study, which are documented in Table 2.

Time (min)



Fluorescein

Fig. 3 (a) Schematic of the synthetic route for PC-COF. (b) The plots of absorbance of dyes by PC-COF versus concentration of the dyes in water. Reproduced with permission from ref. 60. Copyright 2014 the Royal Society of Chemistry. (c) Synthetic strategy for ACA-COF through the Zincke reaction. (d) Removal percentage (%) of uric acid and creatinine via ACA-COF. Reproduced with permission from ref. 44. Copyright 2022, American Chemical Society.

The recent advancement of research has led to the utilization of these vPOPs in the adsorption of uric acid and **Materials Advances** Review

Table 2 Tabular representation of vPOPs used as an adsorbent material for removal of toxic organic dyes from water

S. no.	Name of vPOPs	Organic dye	Organic dye capture capacity (mg g^{-1})	Equilibrium times	Cycle	Ref.
T2.1	iVOFm	Alzarine red S	_	5 min	_	58
		Methyl orange	_	5 min	_	
T2.2	COP_1^{++}	Fluorescein	_	4 min	_	59
T2.3	$COP_1^{\bullet+}$	Rhodamine B	_	60 min		
T2.4	$COP_1^{\vec{0}}$	Nile red	_	60 min		
T2.5	COP_1^{++}	Congo red	928 mg g^{-1}	15 min	_	69
T2.6	C-NSA _{Naph} HCP@Br	Methyl orange	1010 mg g^{-1}	60 min	5	90
T2.7	QUST-iPOP-1	Congo red	1074.9 mg g^{-1}	90 min	_	92
	-	Methyl orange	300 mg g ⁻¹	90 min	_	
T2.8	V-CDP	Congo red	323 mg g ⁻¹	425 min	5	94
		Methyl orange	370 mg g^{-1}	425 min	5	

creatinine which are present in water used for dialysis. Trabolsi et al. 44 synthesized an azacalix[4] arene-based vPOP (ACA-COF) under microwave irradiation (Fig. 3(c)). 44 This is an exceptional instance where a synthetic approach is used to chemically modify an organic macrocycle to limit its ability to change shape and create an ordered substance. The ACA-COF was further used for the removal of uric acid and creatinine from dialyzed water. This application has the capability to save 400 L of water per patient per week. Although it has just gained recognition in the last decade, it has the potential to successfully tackle the issue of water shortage in arid regions worldwide. Their COF exhibited very fast adsorption rates, surpassing previously documented values by many orders of magnitude (Fig. 3(d)).

Inorganic pollutant removal from water. Among the primary inorganic pollutants, the well-known categories include metal cations, oxoanions based on metals or metalloids, and radioactive species. These substances, despite being below the Environmental Protection Agency (EPA) and World Health Organization (WHO) thresholds, are still highly toxic and hazardous to the environment and human health. As a result, there is a strong research focus on selectively removing certain metal species from water-based systems. Although many efficient absorbent substances have been devised, the existing materials have some restrictions, necessitating the development of new, more dependable alternatives.⁶¹ These replacements should inhibit swelling, contain readily available chelating or ion exchange sites, offer a high capacity for saturation or exchange, and have rapid kinetics. In this context, vPOPs have demonstrated outstanding performance in efficiently extracting these pollutants from contaminated water systems. This is attributed to their tunable nature, regulated pore sizes, exchangeable anions and impressive chemical stability.⁶²

Oxoanion removal from water

The escalating phenomenon of urbanization and rapid industrial growth is leading to an increased influx of harmful contaminants into freshwater reservoirs. The Environment Protection Agency (EPA) has identified specific metal or metalloid-based oxoanions, such as chromate (CrO₄²⁻), pertechnetate (TcO₄⁻), perrhenate (ReO₄⁻), arsenate (AsO₄²⁻), among others, classifying them as potential hazardous

inorganic pollutants in wastewater and placing them on a priority list. 63 The Environmental Protection Agency (EPA) has recognized metalloid-derived oxoanions (CrO₄²⁻, TcO₄⁻, ReO₄⁻, AsO₄²⁻) as harmful inorganic pollutants in wastewater, leading to an increasing need for clean water. Hence, wastewater remediation is crucial, and purification methods such as adsorption and ion exchange are emerging as promising alternatives to conventional approaches. In this context, vPOPs are also considered as very promising adsorbent materials to remove metalloid contaminants from water bodies due to their chelating or ion-exchange properties, and are quite favoured because of their cost, user-friendly nature, and ability to minimize the production of dangerous secondary species.⁶⁴ In this regard, vPOPs have been specifically investigated for their efficacy in selectively capturing oxoanions. It is worth noting that due to the robust electrostatic attraction between the mesoporous structure of cationic vPOPs and free replaceable counter anions, various vPOPs have been reported for effectively capturing anionic oxo-pollutants, which are mentioned in Table 3. Among them, triazine-based vPOPs were very efficient for oxoanion removal. Ghosh et al. successfully detoxified wastewater by selectively eliminating various metal-based oxoanions by using triazine based vPOPs (compound-1) (Fig. 4(a)).46 Compound-1, which was synthesized through the solvothermal assisted Zincke reaction, showed remarkable chemical stability. The vPOPs included mobile exchangeable chloride ions, creating an optimal platform for removing toxic oxoanions from water. Compound-1 exhibited strong adsorption capabilities by selectively extracting the carcinogenic ReO₄ ions from water (Fig. 4(b)–(g)). Additionally, to assess real-time effectiveness, an experiment capturing oxoanions through column exchange was conducted. Recently the same group reported the same viologen compound but in the macroporous form, which is discussed in the organic pollutants removal from water section.58 In the same paper, they also checked oxoanion removal through iVOFm and demonstrated exceptionally rapid removal rates for oxoanions (approximately 99% for KMnO₄ and around 97% for KReO₄ within a 30 s timeframe) (Fig. 3(b) and (c)).

In a very recent report, the tetra aza macrocycle containing vPOP was considered as a very potential adsorbent material for separating TcO₄⁻ and ReO₄⁻ from wastewater. ⁹⁹Tc is a radioactive element that releases beta particles. It has a significant

Tabular representation of vPOPs used as an adsorbent material for removal of toxic oxognions from water

		Kinetic study				
S. no.	Name of vPOPs	Time for oxoanion removal	% of oxoanion removal	Oxoanion capture capacity (mg g^{-1})	Selectivity	Ref.
$Cr_2O_7^{2-}$ r	emoval					
T3a.1	C-NSA _{Naph} HCP@Br	60 min	95%	745	F^- , Cl^- , Br^- , $ClO_3^ NO_3$, CO_3^{2-} and PO_4^{3-}	90
T3a.2.	IISERP-POF9	60 min	77%	128.10	Cl^{-} , ClO_4^{-} , and SO_4^{2-} Cl^{-} , ClO_4^{-} , and SO_4^{2-}	83
T3a.3.	IISERP-POF10	60 min	78%	125.21	Cl^- , ClO_4^- , and SO_4^{2-}	
T3a.4.	IISERP-POF11	60 min	81%	131.22	Cl^{-} , $\mathrm{ClO_4}^{-}$, and $\mathrm{SO_4}^{2-}$	
T3a.5.	COP_1^{++}	15 min	95%	_	_	70
T3a.6.	CON-1	60 min	98%	293	_	93
CrO ₄ ²⁻ re	emoval					
T3b.1.	Compound-1	30 min	98.25%	133	Cl ⁻ , NO ₃ ⁻ , Br ⁻ , SO ₄ ²⁻	46
T3b.2.	iCOF-2	60 min	99%	253	Cl^{-} , NO_{3}^{-} , Br^{-} , SO_{4}^{2-}	91
$\mathrm{MnO_4}^-$ re	emoval					
T3c.1	Compound-1	5 min	99.9%	297.3	Cl ⁻ , NO ₃ ⁻ , Br ⁻ , SO ₄ ²⁻	46
T3c.2	IISERP-POF9	60 min	99%	110.53	Cl^- , ClO_4^- , and SO_4^{2-}	83
T3c.3	IISERP-POF10	60 min	97%	103.11	Cl^- , ClO_4^- , and SO_4^{2-}	
T3c.4	IISERP-POF11	60 min	98%	113.81	Cl^- , ClO_4^- , and $SO_4^{\ 2-}$	
T3c.5	iVOFm	30 s	99%	_	_	58
T3c.6	COP_1^{++}	<1 min	99%	_	_	70
T3c.7	iCOF-2	60 min	99%	334	Cl ⁻ , NO ₃ ⁻ , Br ⁻ , SO ₄ ²⁻	91
T3c.8	QUST-iPOP-1	8 min	99%	514	_	92
ReO ₄ rei	moval					
T3d.1	Compound-1	60 min	>80%	517	Cl ⁻ , NO ₃ ⁻ , Br ⁻ , SO ₄ ²⁻ NO ₃ ⁻ , SO ₄ ²⁻ , PO ₄ ³⁻ , CO ₃ ²⁻	46
T3d.2	TFPM-BDNP	1 min	90%	998.26	NO ₃ ⁻ , SO ₄ ²⁻ , PO ₄ ³⁻ , CO ₃ ²⁻	67
T3d.3	TZ-PAF	_	_	982	NO_3^- , SO_4^{2-} , $Cl^-H_2PO_4$	66
T3d.4	VBCOP	5 min	98%	444	Cl ⁻ , NO ₃ ⁻ , SO ₄ ²⁻	65
T3d.5	iVOFm	30 s	97%	_	_	58
T3d.6	COP_1^{++}	30 min	99%	_	_	70
T3d.7	SCU-COF-1	1 min	99%	367	$\mathrm{NO_3}^-$ and $\mathrm{SO_4}^{2-}$	86

fission output and a lengthy half-life. The prompt removal of ⁹⁹Te from liquefied radioactive waste is essential due to its intrinsic potential for causing harm to humans. On the other hand, Re is also considered as a carcinogenic material. In this report, Xia et al. synthesized a tetraaza macrocycle containing vPOP through the solvothermal-assisted Zincke reaction, named VBCOP (Fig. 4(h)).65 This material has great potential as an adsorbent for the absorption of ReO₄⁻/TcO₄⁻, demonstrating exceptional adsorption properties such as fast adsorption rate, high adsorption capacity, excellent selectivity, and efficient regeneration (Fig. 4(i) and (j)). This efficient adsorption process is primarily governed by ion-exchange mechanisms. In addition, they demonstrated the new sequestration of Re(IV) by including a malleable tetraaza macrocycle ligand inside the framework architecture for the first time. The use of EXAFS and XPS analysis reveals that VBCOP⁰ has the ability to create a compound with Re(IV), indicating its potential use in eliminating soluble low-valent Tc species from radioactive wastewater. In summary, VBCOP showed promise in effectively treating both high-valent and low-valent Tc in nuclear effluent. The same group reported a diamond-like topological vPOP named TZ-PAF, for efficient remediation of radioactive TcO₄ from wastewater. TZ-PAF was solvothermally synthesized via the Zincke reaction (Fig. 4(k)).⁶⁶

The TZ-PAF that was synthesized had exceptional resistance to acids and high thermal environment. The material showed rapid anion-exchange kinetics and a high capacity for adsorption (982 mg g⁻¹ for ReO₄⁻), which may be ascribed to its low-

density structure and the presence of many cationic pyridinium rings that act as sites for anion exchange (Fig. 4(k)-(m)). In addition, TZ-PAF had the greatest capacity for removing ${\rm TcO_4}^-$, with a $K_{\rm d}$ value of 5.02×10^6 mL g⁻¹. It also exhibited exceptional reusability for extracting TcO4- from both extremely acidic media and low-activity wastewater streams. Hence, the dia-topology TZ-PAF has successfully addressed the drawbacks of vPOPs, including their susceptibility to acid damage and limited ability to absorb TcO₄-/ReO₄-. As a result, it has emerged as a promising option for efficiently and completely eliminating ReO₄ from nuclear wastes. This paper presents a novel method for creating very stable sorbents, which are very efficient for TcO₄ adsorption.

Qui et al. recently documented, for the first time, the synthesis of three-dimensional viologen-based covalent organic frameworks (Fig. 4(n)).67 They have successfully produced a novel 3D ionic covalent organic framework (iCOF), named TFAM-BDNP, through the microwave-assisted Zincke reaction. TFAM-BDNP demonstrates exceptionally rapid response times, a high adsorption rate, superior selectivity, and impressive resistance to changes in pH, along with the ability to be reused for the removal of TcO₄⁻/ReO₄⁻. Owing to its outstanding stability, open hydrophobic channels, and high charge density, TFAM-BDNP presents itself as a promising candidate for the removal of TcO₄⁻/ReO₄⁻ (Fig. 4(o) and (p)). This research not only diversifies the structural variations of 3D covalent organic frameworks but also broadens their applications in processes related to the disposal of nuclear waste.

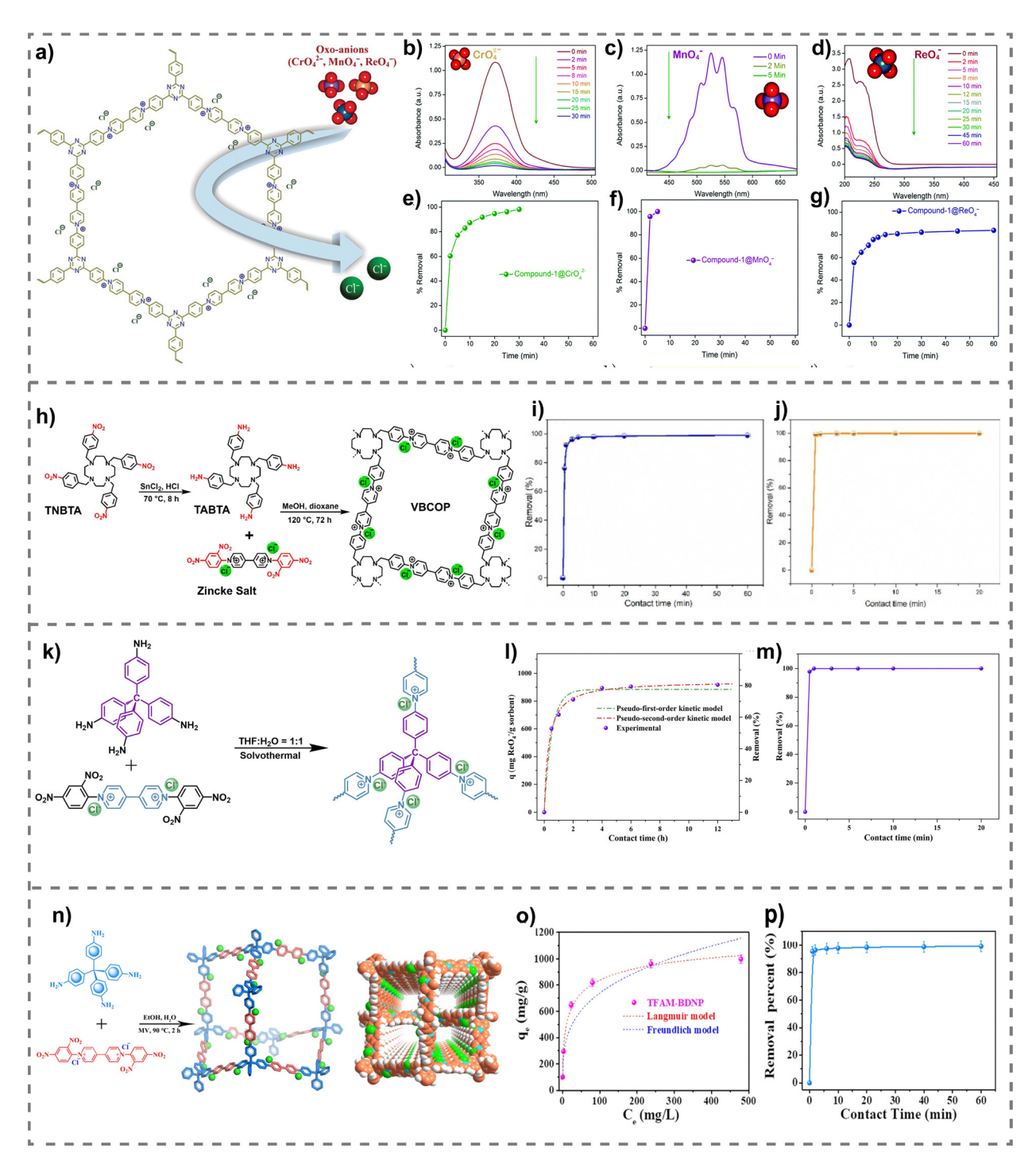


Fig. 4 (a) Schematic representation of the oxo-anion capture by compound-1. (b)-(g) Kinetic studies of removal of all oxoanions by compound-1. Reproduced with permission from ref. 46. Copyright 2014 the Royal Society of Chemistry. (h) Schematic representation of the synthesis of VBCOP. (I) Effect of contact time on the removal efficiency of Re(vii) by VBCOP ($C_0 = 45 \text{ mg L}^{-1}$, pH = 7). (j) Effect of contact time on the removal efficiency of 99Tc(vii) by VBCOP. Reproduced with permission from ref. 65. Copyright 2018, Elsevier. (k) Schematic of the synthetic route for TZ-PAF. (l) and (m) Sorption kinetic investigations of TZ-PAF for ReO₄⁻ uptake. Reproduced with permission from ref. 66 Copyright 2018, Elsevier. (n) Synthetic pathway of 3D iCOF (TFAM-BDNP). (o) and (p) Adsorption kinetics and adsorption isotherm of TFAM-BDNP for ReO₄⁻ capture. Reproduced with permission from ref. 67. Copyright 2018, Elsevier.

I₂ uptake. Iodine is considered one of the most hazardous elements and can cause very serious health issues due to its radioactive decay.²⁸ So, the removal of iodine from water bodies is one of the most important considerations for healthy mankind. Over the years, iodine removal has become one of the extensively researched areas. Among all the iodineadsorption materials, vPOPs possess extremely strong iodinecapturing capabilities due to their redox switch and

quaternized nitrogen atoms.⁶⁸ The researchers investigated the impact of various redox states of viologen on iodine absorption in many vPOPs with distinct core structures, including phosphazene, calixarene, 1,3,5-tris(4-aminophenyl)benzene (TAPB), etc. The findings are impacted by several factors, such as the basic features, presence of viologen counterions, porosity, redox state, and the presence of existing iodine sorption sites. The inclusion of large counterions like PF₆⁻ limits the available surface area for iodine interaction, leading to a reduction in absorption efficiency of up to 30%. vPOPs (COP₁⁺⁺ and COP2⁺⁺) that are fully reduced and neutral possess a significant capacity to absorb iodine, resulting in a maximum increase in mass of up to 380% (Fig. 5(g)). 69 The radical cationic vPOPs act as Lewis bases and are likely responsible for the enhanced interactions with Lewis acids I₂ and I₃. Additionally, neutral vPOPs (COP₁ and COP2) lack counterions, perhaps increasing the available surface area for iodine to engage with the framework (Fig. 5(a) and (d)).⁷⁰ Highly stable radical cationic vPOPs (COP₁⁺ and COP2 have the potential to engage in a series of reductionoxidation reactions with polyiodides and formed dicationic vPOP and I₃ (Fig. 5(h)) This process provides vPOPs a substantial ability for absorbing iodine vapor. 69 The enduring nature of the radical cationic viologen is crucial for facilitating these reactions.

The above-mentioned discussion is a common overview of how the redox-active behaviour of vPOPs affected the iodine adsorption process. The 1st synthesized vPOPs gel (COGF), through the solvothermal assisted Zincke reaction, exhibited remarkable iodine adsorption efficiency (Fig. 5(e)). 43 The same research group reported viologen and pyrene-based covalent organic nanosheets (CONs) and covalent organic tubes (COTs) for iodine adsorption in the solution phase as well as the vapor phase (Fig. 5(i)). COTs exhibited high efficiency in iodine adsorption in both phases, as the presence of triple bonds and more cationic surface leads to fast iodine capture in COTs (Fig. 5(j) and (k)).89

Gas storage and separation

The proliferation of modern industrial processes has resulted in the substantial emission of greenhouse gases, most notably carbon dioxide (CO2), which presents a considerable peril to the state of the environment.⁷¹ Therefore, it is crucial to prioritize the development of renewable energy sources and implement efficient strategies for storing and converting greenhouse gases. The high surface areas of vPOPs, which are essential for gas adsorption materials that interact with gas molecules via noncovalent means, have prompted investigations into their potential as CO2 adsorbents.72 vPOPs frequently distinguish themselves due to their exceptional stability, economical nature, and straightforward synthesis. Nevertheless, the adsorption capabilities of vPOPs have been predominantly evaluated in less severe environments, and they have been widely employed in the storage and conversion of greenhouse gases. Although there have been conjectures regarding the cationic charge of viologen and the potential pore-blocking effect of

counterions restricting the porosity of viologen-based POPs, there have been numerous reports of materials with considerable surface areas.⁷³ Dicationic viologens, in conjunction with their corresponding counterions in vPOPs, are capable of forming electrostatic interactions with CO2 by virtue of their polar functional groups which enhances the affinity of the material for CO2. Coskun et al. reported a vPOP (PCPs) synthesized via the Sonogashira-Hagihara coupling reaction to examine the effect of exchangeable counterions on the adsorption of CO₂ (Fig. 6(a)).⁷⁴ The incorporation of bulkier counterions such as BF4 or PF6 resulted in a reduction in the material's surface area. However, BF4 and PF6 may function as Lewis bases, which somewhat compensates for their CO₂ absorption capability, although at the expense of having comparatively lower surface areas (Fig. 6(b) and (c)). Recent observations from the same research group indicate that substituting a bromide counterion for chloride improves CO₂ uptake in a vPOP (cCTF) containing a Zincke reaction-fabricated polyhedral oligomeric silsesquioxane core.⁷⁵ At elevated temperatures, gas adsorption diminishes, irrespective of the type of counterion. For CO2 adsorption, a covalent triazine framework (cCTF) was utilized, which consisted of a porous viologen substituted with cyanophenyl, as illustrated in Fig. 6(d). The reaction temperature during the synthesis process had a significant impact on the surface areas of these frameworks, with the highest value of 1247 m² g⁻¹ occurring at 500 °C. The compound exhibited highest CO₂ adsorption capacity (133 mg g⁻¹) among all other vPOPs. (Fig. 6(e)-(h)). The authors hypothesized that the cationic groups attached to viologen groups increased the CO2 absorption capacity of vPOPs by as much as fivefold, in comparison with other triazine framework-based materials that possess comparable surface areas. D'Alessandro et al. studied the effect of the redox behavior of the viologen moiety on CO₂ uptake experimentally as well as theoretically.76 After the twoelectron reduction of dicationic viologen, the gas uptake capacity decreases, from 0.92 mmol g^{-1} (approximately 40.5 mg g^{-1}) to 0.67 mmol g⁻¹ (approximately 29.5 mg g⁻¹) in POP-V1, and from 1.27 mmol g^{-1} (approximately 55.9 mg g^{-1}) to 1.09 mmol g^{-1} (approximately 48.0 mg g^{-1}) in POP-V2 (Table 4). The authors posit (based on their theoretical modelling) that Cl⁻ counterions have paramount importance in enhancing the interactions with CO2 molecules. The decrease in CO2 absorption is a direct consequence of the elimination of the counterion during reduction from dicationic state to its neutral state. As a result of these investigations as a whole, it is clear that the charge on viologen and its chloride counterions is vital for covalent materials based on viologen to maximize their CO2 adsorption capacity. Nowadays, researchers are finding several innovative ways or concepts to improve the catalytic efficiency of vPOPs for CO₂ fixation (Table 4).

The incorporation of halogen bond donors (HBDs) in the frame of vPOPs leads to a new class of materials that can be used as a catalyst for CO₂ fixation. Utilizing this new concept Chen et al. synthesized HBD-incorporated hybrid vPOPs, named V-iPHPs (Fig. 7(c)), and used these materials for catalytic CO₂ fixation.⁷⁷ V-iPHPs were synthesized through the

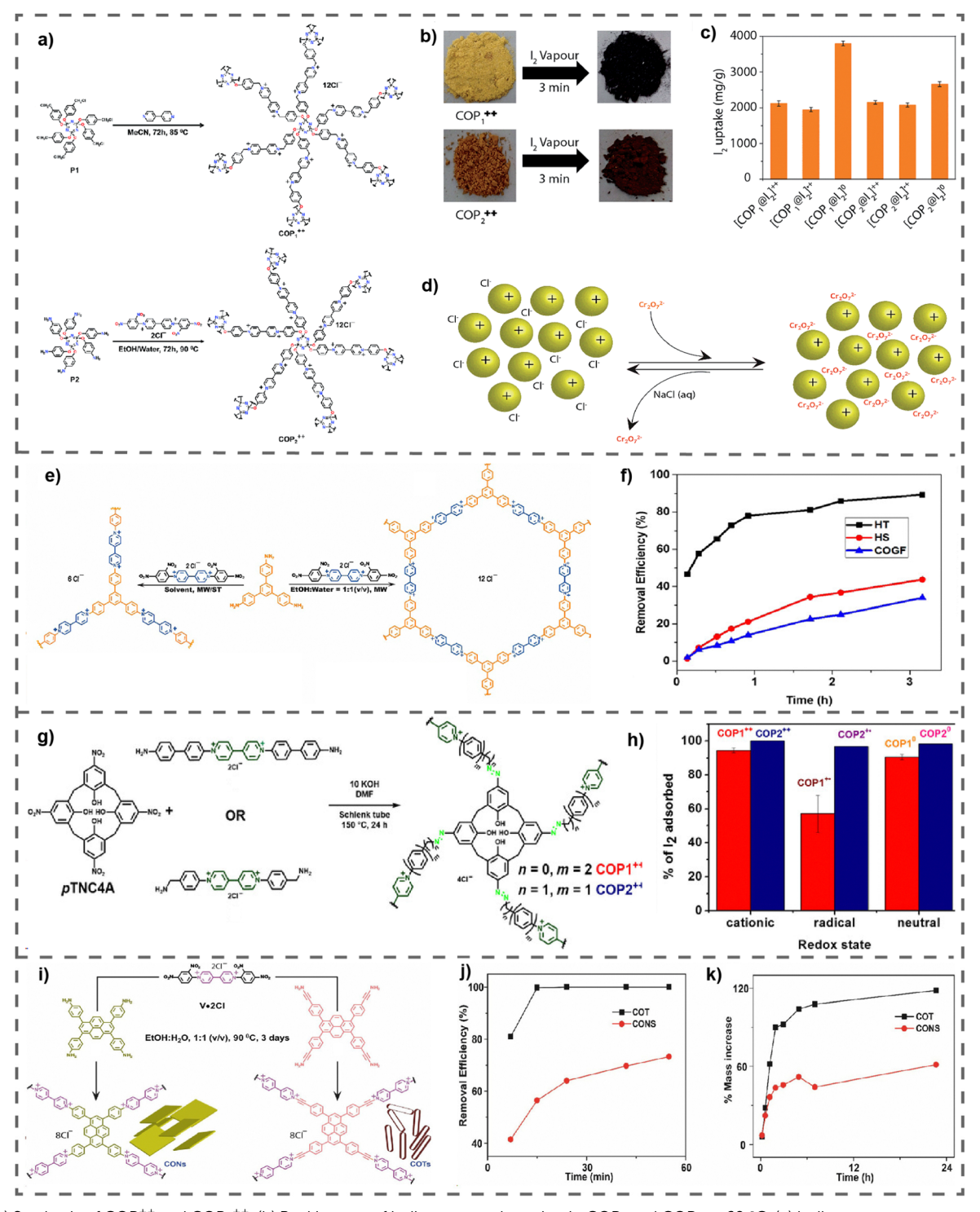


Fig. 5 (a) Synthesis of COP_1^{++} and COP_2^{++} . (b) Real images of iodine vapor adsorption in COP_1 and COP_2 at 60 °C. (c) Iodine vapor capture capacities of COP_1 and COP_2 in three different redox states. (d) Schematic representation of anion removal $(MnO_4^-, Cr_2O_7^{2-})$ by anion exchange, where yellow spheres represent polymer particles (COP1 and COP2). Reproduced with permission from ref. 70. Copyright 2014 the Royal Society of Chemistry. (e) Synthesis of the hollow sphere (HS) and hollow tube (HT) via the solvothermal synthesis approach and the covalent organic gel framework (COGF) via the microwave synthesis approach. (f) Graph of % removal of I2 from a 1 mM solution in cyclohexane over time by HT, HS and COGF. Reproduced with permission from ref. 43. Copyright 2022, American Chemical Society. (g) Synthesis of COP1++ and COP2++. (h) Solution-phase iodine adsorption by the three redox states of COP1 and COP2. Reproduced with permission from ref. 69. Copyright 2022 Wiley-VCH. (i) Synthesis of CONs and COTs, (j) and (k) lodine adsorption experiments. Reproduced with permission from ref. 89. Copyright 2022 Wiley-VCH.

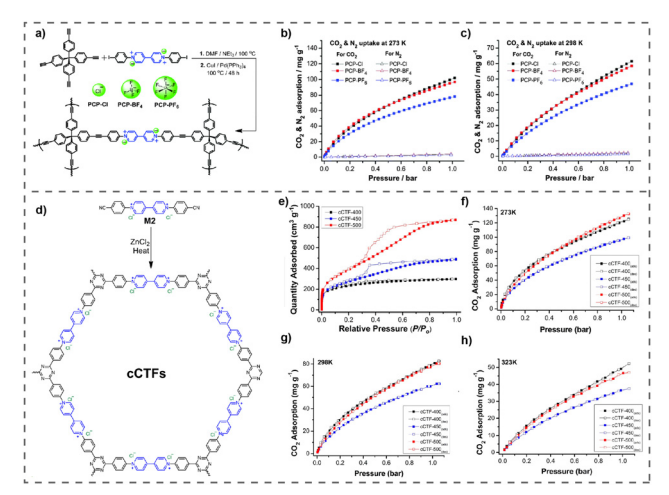


Fig. 6 (a) The synthesis of PCP-Cl, PCP-BF $_4$ and PCP-PF $_6$. CO $_2$ and N $_2$ uptake isotherms of PCPs measured up to 1 bar at (b) 273 K and (c) 298 K. Reproduced with permission from ref. 74. Copyright 2014 the Royal Society of Chemistry. (d) Synthesis route for cCTFs. CO2 adsorption isotherms of cCTFs at (e) 273 K, (f) 298 K, and (g) 323 K. (H) The isosteric heat of adsorption (Q_{st}) plots for CO₂. Reproduced with permission from ref. 75. Copyright 2022, American Chemical Society.

solvothermal assisted Heck reaction. V-iPHPs have tunable surface areas and pore volumes, and adjustable ionic sites. They exhibit metal-free heterogeneous catalytic activities in CO₂ fixation with diverse epoxide substrates under mild conditions (Fig. 7(d)). The catalyst's remarkable performance is credited to synergistic catalysis sites, ample mesoporosity, and the hydrophobic reaction microenvironment. Wang et al. also demonstrated that POSS and viologen-linked vPOPs (V-PCIF-X, X = Cl, Br) function as a metal-free catalyst and adsorbent of exceptional efficacy, enabling the concurrent capture and conversion of CO₂ (Fig. 7(a)). Due to their high surface area, tunable pore size and specifically presence of mobile Si-OH, these vPOPs are

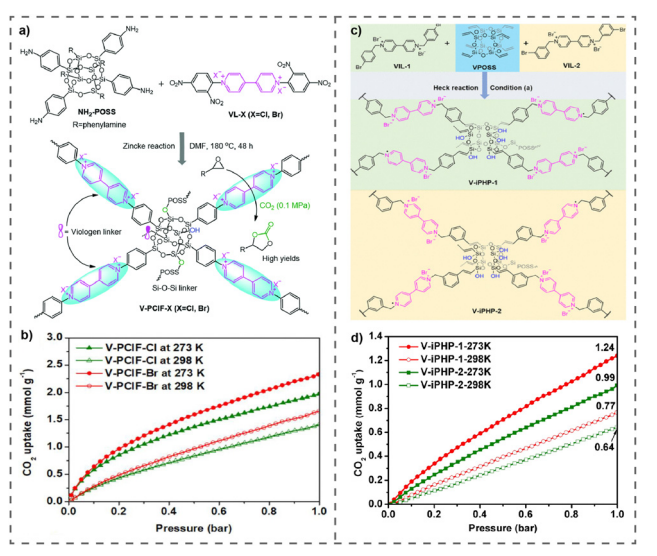


Fig. 7 (a) The synthesis of V-PCIF-X (X = Cl, Br), (b) CO_2 uptake of V-PCIF-Cl and V-PCIF-Br at 273 K and 298 K. Reproduced with permission from ref. 78. Copyright 2014 the Royal Society of Chemistry. (c) Synthetic route for V-iPHP-1 and V-iPHP-2, (d) CO₂ uptake of V-iPHP-1 and V-iPHP-2 at 273 K and 298 K. Reproduced with permission from ref. 77. Copyright 2022, American Chemical Society.

remarkable CO₂ adsorbents (Fig. 7(b)) and are denoted as excellent metal-free catalysts for the conversion of CO₂. 78

Energy storage and conversion

Renewable energy sources, such as wind, solar, water, and hydrogen energy, which are clean and environmentally friendly, have garnered significant interest. However, the availability of many renewable resources is heavily influenced by geographical location, season, and climate, often requiring large-scale storage devices, unlike conventional fossil fuels. To address these challenges, there is a growing demand for advanced

Table 4 Tabular representation of vPOPs for CO₂ gas uptake

S. no.	vPOPs	BET surface area	CO_2 uptake (mmol g^{-1})			Pressure	
		$(S_{\text{BET}}) \text{ m}^2 \text{ g}^{-1}$	273 K	298 K	323 K	(bar)	Ref.
T4.1	cCTF-400	744	2.86	1.88	1.18	1	75
T4.2	cCTF-450	861	2.25	1.40	0.86	1	
T4.3	cCTF-500	1247	3.02	1.82	1.06	1	
T4.4	V-PCIF-Br	174	1.97	1.41	_	1	78
T4.5	V-PCIF-Cl	383	2.33	1.66	_	1	
T4.7	POP-V1	812	_	0.92	_	1.1	76
T4.8	Red-POP-V1	606	_	0.67	_	1.1	
T4.9	POP-V2	960	_	1.27	_	1.1	
T4.10	Red-POP-V2	591	_	1.09	_	1.1	
T4.11	PCP-Cl	755	2.31	1.39	_	1	74
T4.12	$PCP-BF_4$	586	2.20	1.32	_	1	
T4.13	PCP-PF ₆	433	1.77	1.06	_	1	
T4.14	CCTF-500	1353	_	1.94	_	1	73
T4.15	V-iPHPs	562	1.24	_	_	1	78
T4.16	VIP-Br	38	_	_	_	_	88
T4.17	VIP-Cl	56	_	_	_	_	88
T4.18	H2-ICOP	9	0.96	1.42	0.39	1	95
T4.19	Zn-ICOP	20	0.45	0.89	0.54	1	
T4.20	SYSU-Zn@IL1	38	1.54	0.90	_	1	96

storage and conversion technologies. In recent years, attention has shifted towards new energy devices like batteries and supercapacitors. Viologens and their derivatives are frequently employed in these devices due to their optimal electron accepting capability and favorable redox behavior. 31,79

Very recently our group reported a series of viologen-based covalent organic networks (vCONs) as metal-free bifunctional electrocatalysts for oxygen reduction reaction (ORR) and oxygen evolution reaction (OER).80

Here, we synthesized four vCONs through the solvothermalassisted Zincke reaction, denoted as vGC, vGAC, vMEL and vBPDP, based on triamines used as reactants (Fig. 8(a)). The incorporation of redox-active viologen groups into the extended covalent organic framework was essential for achieving

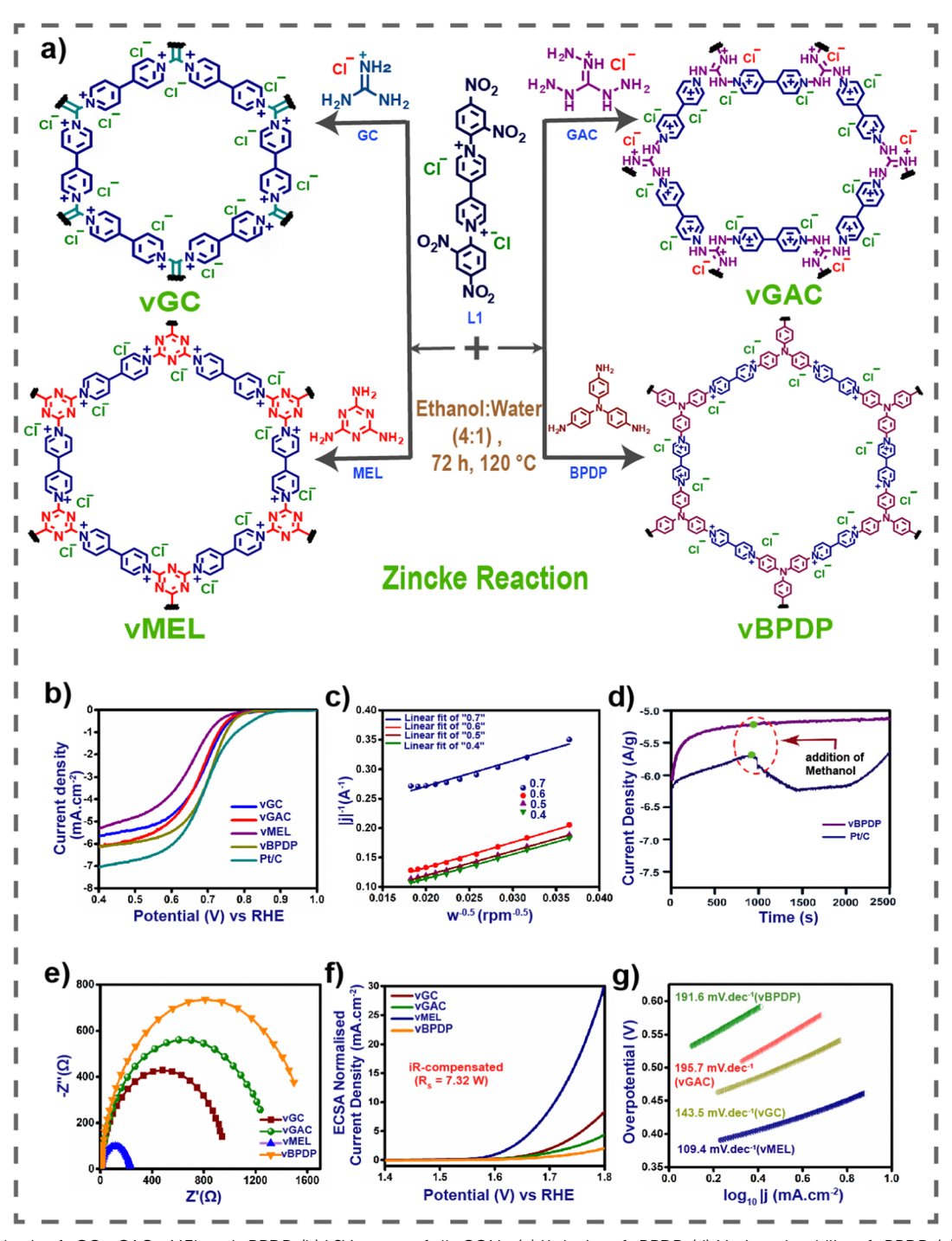


Fig. 8 (a) Synthesis of vGC, vGAC, vMEL and vBPDP. (b) LSV curves of all vCONs. (c) K-L plot of vBPDP. (d) Methanol stability of vBPDP. (e) EIS spectra of all vCONs. (f) LSV curves for the OER of all vCONs. (g) Tafel plots of all vCONs. Reproduced with permission from ref. 80. Copyright 2014 the Royal Society of Chemistry.

exceptional stability in both acidic and basic environments, as well as for demonstrating dual functionality in the oxygen reduction reaction (ORR) and oxygen evolution reaction (OER). The verification was conducted using cyclic voltammetry (CV) curves. Significantly, vBPDP exhibited a remarkable oxygen reduction reaction (ORR) efficiency, achieving a half-wave potential of 0.72 V relative to a reversible hydrogen electrode (RHE) in a 1 M KOH electrolyte (Fig. 8(b)-(e)). However, vMEL demonstrated impressive OER (oxygen evolution reaction) performance, achieving an overpotential of 320 mV at a current density of 10 mA cm⁻² and a Tafel slope of 109.4 mV dec⁻¹ in a 1 M KOH electrolyte solution (Fig. 8(f) and (g)). This research is notable for using unadulterated viologenbased covalent organic networks as bifunctional electrocatalysts (for ORR and OER) without the inclusion of any metallic elements or conductive substances. There is a firm conviction that these particular varieties of vCONs possess the capability and efficiency to function as bifunctional electrocatalysts for ORR and OER. Consequently, these vCONs will be extremely useful in energy storage devices of the upcoming generation.

Wen et al. have effectively synthesized a two-dimensional redox-active cationic covalent triazine network (cCTN) utilizing the solvothermal-assisted Zincke reaction. 45 This network acts as a metal-free electrocatalyst for ORR in order to generate H₂O₂ (Fig. 9(a)). The cCTN electrocatalyst was synthesized with a mesoporous structure, characterized by a pore width ranging from 2 to 10 nm. It has a total nitrogen concentration of 13.3 wt%. This polymer has a reversible two-electron redox mechanism, which is thought to enhance the ORR efficiency for the generation of H₂O₂. The cCTN electrocatalyst exhibits excellent ORR performance and impressive specificity (over 85%) for H₂O₂ production across a broad potential range (0.1-0.7 V) (Fig. 9(b)-(e)). Electron paramagnetic resonance (EPR) tests showed that the viologen units in the cCTN electrocatalysts may initiate the activation of molecular oxygen, resulting in the production of superoxide radicals (O^{2-}) , which support the 2e⁻ pathway of the ORR for the electrochemical synthesis of H2O2. This work presents a novel method for developing metal free electrocatalysts that are extremely specific to producing H₂O₂ from O₂. Current research is dedicated to improving the efficiency and specificity of the cCTN electrocatalyst.

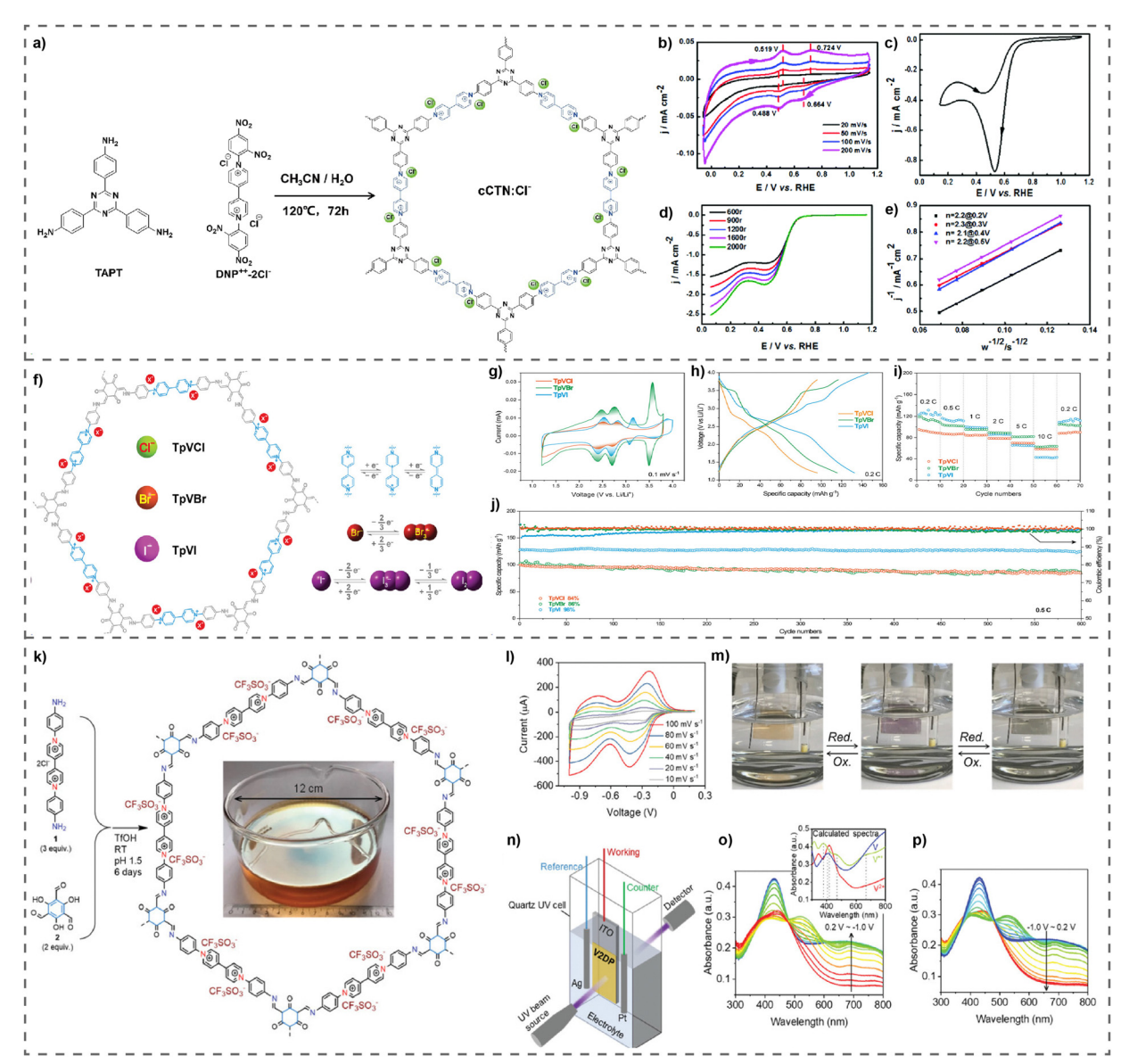
These ionic vPOPs are also recognized as remarkable cathode materials for Li-ion batteries. Recently, Li et al. reported a series of novel cationic vPOPs, denoted as TpVXs (where X = Cl, Br, or I), used as cathode materials in Li-ion batteries (Fig. 9(f)). Halogens which are used in LI-ion batteries serve as efficient cathodic materials but exhibit significantly very poor cycling efficacy.81 The vPOPs (TpVXs) are specifically engineered to feature numerous pores and ionic redox-active components to effectively and durably trap halogen anions accurately and appropriately. The TpVBr and TpVI electrodes demonstrate a notable initial specific capacity of 116 and 132 mA h g⁻¹ at 0.2C, respectively, along with an elevated discharge voltage of around 3.0 V (Fig. 9(g)-(i)). Remarkably, due to their permeable and ionic composition, TpVBr and TpVI exhibit exceptional durability over extended periods of use (86% and 98% capacity preservation after 600 cycles at 0.5C), surpassing the performance of the most advanced halogen electrodes (Fig. 9(j)).81

Viologens recognized as a crucial optoelectronic material have found application in solar cells either as the active chromophore or as materials modified for electrodes. Feng et al. showcase a highly crystalline 2D polymer film with immobilized viologen (V2DP),47 characterized by a dense array of inherent pores and well-defined channels that facilitate the efficient utilization of viologen moieties and ion transport (Fig. 9(k)). Leveraging this, they constructed V2DP-based electrochromic devices (ECDs) demonstrating swift switching speeds (2.8 s for coloration, 1.2 s for bleaching), a high Coulombic efficiency (989 cm² C⁻¹ at 90% of the full switch), and low energy consumption (21.1 μ W cm⁻²) (Fig. 9(l)-(n)). Additionally, the researchers illustrated the integration of these ECDs with transparent solar cells (TSCs), creating energyefficient electrochromic window systems capable of dynamically adjusting light automatically (Fig. 9(o) and (p)). This innovation aligns with intelligent solar spectrum management. Their findings lay the foundation for designing and synthesizing electroactive 2D polymer films for superior smart windows, broadening the possibilities for energy-efficient building applications in the future.

Catalysis

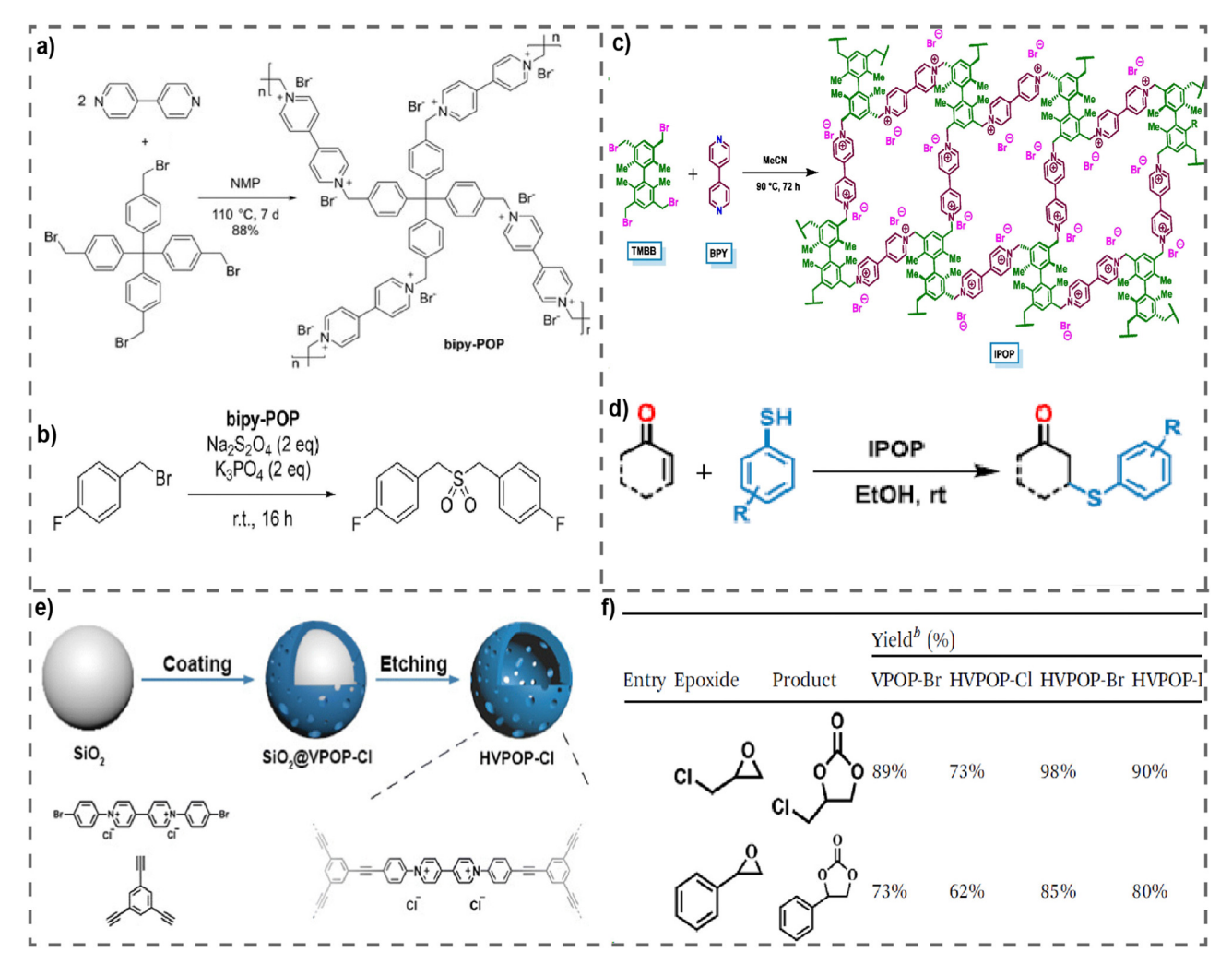
Catalysis is important to facilitate chemical reactions. Catalytic reactions hold considerable importance in the production of numerous industrial compounds and minerals, in addition to their utilization in a diverse array of applications such as pharmaceutical synthesis, environmental remediation, energy generation, and food manufacturing.97,98 Catalysis may be classified into two primary categories: homogeneous catalysis and heterogeneous catalysis. Homogeneous catalysts are characterized by their ability to stay in the same phase as the reactants, whereas heterogeneous catalysts are distinguished by their ability to remain in a separate phase. Homogeneous catalysts, despite their superior activity and selectivity, encounter some constraints such as stability and separation challenges. Consequently, substantial scientific efforts have been dedicated to the creation of heterogeneous catalysts.99 In this regard, vPOPs are one of the most ideal materials for heterogeneous catalysts due to their insolubility in water and organic solvents along with exceptional durability and longevity, hence facilitating advantageous chemical reactions under the conditions of reduced temperatures and pressures, vPOPs exhibit redox chemistry, enabling the transfer of electrons, and forming robust complexes with metal nanoparticles that have a negative charge. Moreover, the counterions of the viologen moiety function as nucleophiles and leaving groups, which helps in enhancing their catalytic efficiency. 100 These insoluble and stable vPOPs were used as heterogeneous catalysts for several reactions such as cycloaddition of CO₂ or CO₂ fixation, debromination, Michael addition of thiols, etc.

In the year of 2019, Li et al. reported an exceptionally stable vPOP, known as bipy-POP (Fig. 10(a)), which was synthesized by reacting 4,4'-bipyridine with tetrakis(4-(bromomethyl)phenyl)methane in N-methylpyrrolidone at a temperature of 110 °C and which was further employed as a heterogeneous catalyst for



(a) Synthesis of cCTN:Cl⁻, (b) CVs of cCTN:Cl⁻, (c) CV of cCTN:Cl⁻ in 0.1 M KOH solution, (d) LSVs of the ORR of cCTN:Cl⁻, and (e) Koutecky-Levich plots at different potentials. Reproduced with permission from ref. 45. Copyright 2014 the Royal Society of Chemistry. (f) Proposed mechanism of TpVXs, electrochemical characterization of TpVXs as cathode materials. (g) CV curves of TpVXs, (h) charge/discharge curves at indicated current densities of TpVXs, and (i) rate performance and (j) cycling stability of TpVXs cathodes. Reproduced with permission from ref. 81. Copyright 2022 Wiley-VCH. (k) Synthesis of the V2DP film. Electrochemical characterization of the V2DP film. (l) CV curves of the V2DP electrode at different scan rates from 10 to 100 mV s⁻¹. (m) Real time images of reversible color changing of the V2DP film. (n) Schematic presentation of the in situ spectroelectrochemical measurement. UV-vis spectral changes of the V2DP electrode recorded during (o) reductive and (p) oxidative processes. Reproduced with permission from ref. 47. Copyright 2022 Wiley-VCH.

the debromination coupling reaction. 101 The bipy-POP catalyst has shown significant efficacy in facilitating the reductive debromination of several benzyl bromides in N,N-dimethylformamide, using dithionite as the reductive reagent. The reactions preferentially produced dibenzyl sulfone derivatives for substrates that had an electron-donating group on the benzene ring (Fig. 10(b)). In general, the presence of an electron-withdrawing group on the benzene ring in substrates has been seen to result in the formation of coupling products, namely ethane derivatives. In some cases, substrates containing F, Cl, or CF₃ were seen to have a preference for the production of sulfone derivatives. The study investigated the recyclability of bipy-POP in the catalysis of the reaction between (4-fluorophenyl) methyl bromide and diphenylmethyl bromide, resulting in the formation of sulfone or ethane derivatives. The results indicated that, even after 40 cycles of repeated use, the heterogeneous catalysis did not demonstrate a significant decrease in activity. Recently, a novel vPOP named IPOP was employed as a heterogeneous catalyst for the Michael addition of thiols to α,β-unsaturated carbonyl compounds (Fig. 10(c)). 102 IPOP was



(a) Synthesis of bipy-POP, (b) catalyst bipy-POP used for debromination coupling reaction for formation of sulfone. Reproduced with permission from ref. 101. Copyright 2022 Wiley-VCH. (c) Synthesis of IPOP, (d) IPOP-catalysed Michael addition of thiols to a,b-unsaturated carbonyl compounds. Reproduced with permission from ref. 102. Copyright 2018, Elsevier. (e) Schematic diagram of the synthesis route for HVPOP-CI, (f) performance of comparative materials in the cycloaddition of CO₂. Reproduced with permission from ref. 103. Copyright 2014 the Royal Society of Chemistry.

synthesized through the Menshutkin reaction by using a twisted biaryl (TMBB) as the monomer (Fig. 10(c)). IPOP exhibits thermal stability and lacks solubility in water as well as in commonly used organic solvents such as MeOH, MeCN, EtOH, DCM, and others. IPOP has capabilities similar to the phase-transfer quaternary ammonium salt tetra-n-butylammonium bromide (TBAB), due to the inclusion of cationic sites and counter bromide anions in its polymeric matrix. This characteristic enables IPOP to be used as a reusable heterogeneous catalyst for organic transformations. IPOP is a very effective catalyst for the Michael addition of thiols to α,β -unsaturated carbonyl compounds (Fig. 10(d)). This process allows for the production of organosulfur compounds, namely b-arylthioketones, with high yields in isolation. Comparably, it has been demonstrated that IPOP can serve as a recyclable heterogeneous catalyst for the easy production of biscoumarins. These compounds belong to a significant category of molecular systems that demonstrate diverse biological properties, including anti-coagulant, antianthelmintic, anti-HIV, anti-bacterial, anti-oxidant, anti-cancer,

and so on. Therefore, a new, effective, and environmentally friendly method has been created to synthesize b-arylthioketones and biscoumarins by imitating the phase transfer of quaternary ammonium salts. IPOP can be used as a heterogeneous catalyst for a minimum of 10 catalytic cycles without any decrease in catalytic activity.

It has also been reported that vPOPs can play a direct catalytic role in fixing CO2 into cyclic carbonates from a variety of epoxide-starting materials. The mechanisms by which these reactions occur are as follows: at the very first step, the epoxide is activated via hydrogen bonding with the α-protons of viologen and the epoxide ring is then exposed by a nucleophilic attack of Cl ions. The resulting intermediate undergoes recyclization upon reaction with CO₂, whereas Cl⁻ functions as a leaving group. 72 Based on this mechanism, using the Sonogashira-Hagihara cross-coupling reaction, a viologen-based porous organic polymer featuring a hollow structure and active anions was synthesized (named VPOP-Cl) from two basic monomers (Fig. 10(e)). 103 This material exhibited exceptional

Materials Advances Review

performance in the catalytic cycloaddition of CO2. The pore properties of pristine VPOP-Cl were modified by alterations in micromorphology, and the exchange of anions enhanced its catalytic performance. Additionally, the modified HVPOP-Br demonstrated excellent reusability and catalytic performance in a solvent-free, metal-free reaction system devoid of cocatalysts. A substantial enhancement in the catalytic efficiency of CO2 cycloaddition was achieved through the modification of the microscopic structure and the exchange of anions (Fig. 10(f)). This approach may offer suggestions for enhancing the catalytic performance of POPs utilizing polymers with a basic structure. Similarly, Chen et al. reported a series of crystalline vPOPs (designated VIP-X, X = Cl or Br) that have acted as the metal-free heterogeneous catalyst for the degradation of CO2. In the synthesis of cyclic carbonate via CO2 cycloaddition with epichlorohydrin at atmospheric pressure (1 bar) and a low temperature (40 °C), the optimal catalyst VIP-Br produced a high yield of 99%. 88 Furthermore, under mild conditions, other diverse epoxides could also be converted into cyclic carbonates. Additionally, the catalyst VIP-Br exhibited favorable stability and could be readily isolated for reuse. The exceptional catalytic performance may be ascribed to the synergistic influence of the enriched bromine anion species and the accessible hydroxyl

(OH) groups that originate from water molecules that are Hbonded. The same group reported HBD-incorporated hybrid vPOPs, named V-iPHPs (Fig. 7(c)), that were used for catalytic CO₂ fixation.⁷⁷ The V-iPHP-1 catalyst has exceptional metal-free heterogeneous catalytic properties in the process of CO2 fixation using various epoxide substrates, even under very gentle circumstances. Moreover, the heterogeneous catalyst V-iPHP-1 exhibits a high degree of recoverability and impressive reusability. The exceptional catalytic performance may be attributed to the synergistic catalytic effects resulting from the presence of hydrogen bond donors, namely Si-OH groups and Br⁻ anions, as well as the abundance of mesopores and the hydrophobic reaction microenvironment.

Photocatalyst. Photocatalysis is the process by which substances that are classified as photocatalysts modify the rate of chemical reactions when exposed to light or sunlight. Visiblelight-driven photocatalytic technology, which converts solar energy to chemical energy, offers the potential for chemical transformations such as pollutant removal, water splitting, and hydrogen evolution. Therefore, creating effective photocatalysts with high catalytic activity is crucial. 104,105 Eventually, vPOPs are considered as an ideal photocatalyst for the photocatalysis phenomenon due to the redox-active nature of the viologen

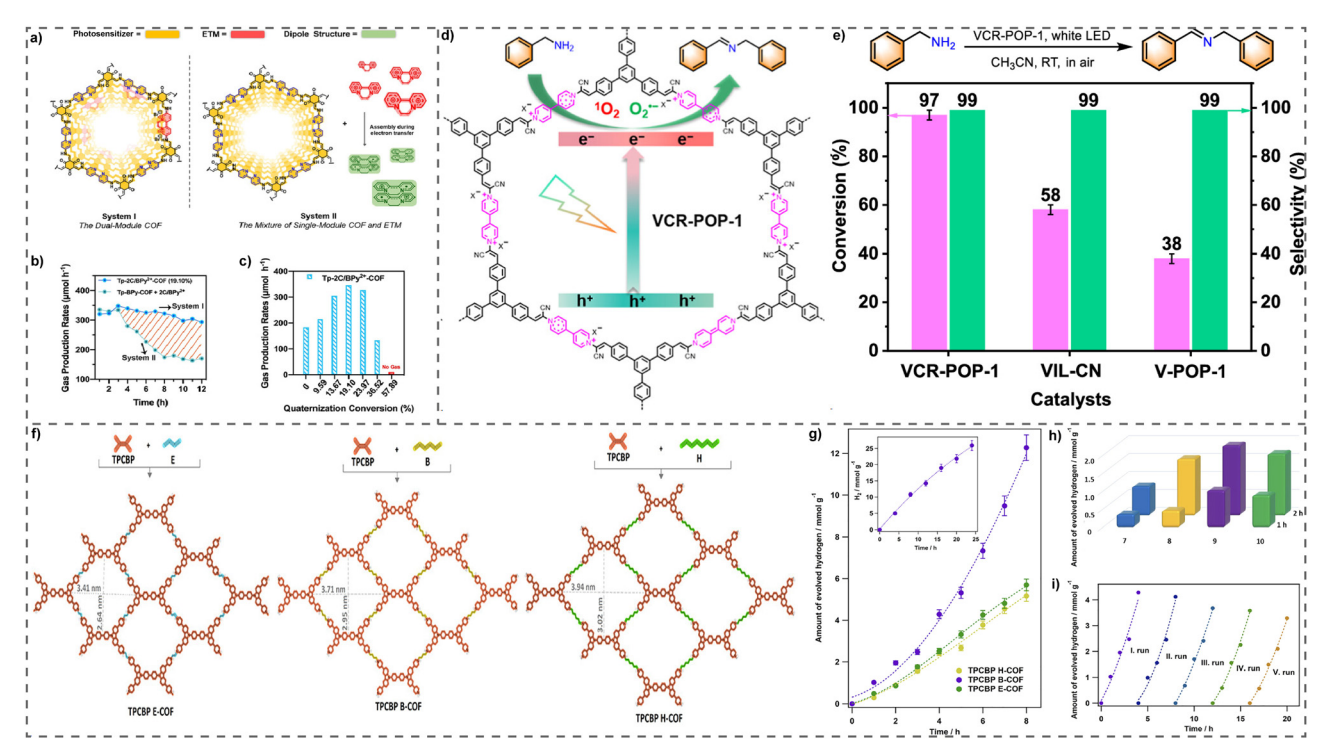


Fig. 11 (a) Schematic diagram of the dual-module COF (System I) and the mixture of single-module COF with unembedded ETM (System II). (b) The hydrogen evolution test of the integrated $Tp-2C/BPy^{2+}-COF$ (19.10%) and the bare Tp-BPy-COF mixed with additional $2C/BPy^{2+}$ used as an ETM under visible-light irradiation. The orange integral area roughly reflects the hydrogen evolution difference between the two photocatalytic systems. (c) HERs of Tp-2CPBy²⁺-COF (10 mg) with different quaternization conversions. Reproduced with permission from ref. 107. Copyright 2022 Wiley-VCH. (d) Schematic representation of photocatalytic oxidative coupling of benzylamine through VCR-POP-1. (e) Photocatalytic performance in white-lightdriven photocatalytic oxidative coupling of benzylamine into imine over different catalysts VCR-POP-1, VIL-CN, and V-POP-1. Reproduced with permission from ref. 110. Copyright 2022, American Chemical Society. (f) Schematic representation of TPCBP X-COF [X = ethyl (E), butyl (B), and hexyl (H)] structures. (q) Photocatalytic hydrogen evolution activities of TPCBP X-COFs. (h) pH effect of TEOA. (i) Photocatalytic stability test of TPCBP X-COFs. Reproduced with permission from ref. 108. Copyright 2022, American Chemical Society

moiety and radical formation tendency. Recently, radical porous organic polymers (RPOPs)106 are emerging as potential materials for photocatalysis and vPOPs are considered as one kind of RPOP because vPOPs form easily stable radical cations by undergoing one electron reduction (Scheme 1). Viologen and its derivatives facilitate the rapid transfer of electrons from photosensitizers to active sites by functioning as electrontransfer mediators (ETMs). However, the electron-transfer capability is frequently impeded by the formation of a stable dipole structure due to the coupling between viologen-derived ETMs that contain cationic radicals; this results in the restriction of the electron-transfer process. To address this issue, Guo et al. installed a cyclic diquat in a 2,2'-bipyridinium covalent organic framework via a quaternization reaction (Fig. 11(a)). 107 Cyclic diquats are known for viologen-derived ETMs. 108 By the synergistic influence of steric hindrance and electrostatic repulsion, these entities are selectively immobilized on distinct sites and kept apart. This prevents the development of stable p-stacked cationic radicals throughout the electron transfer procedure. The conductivity and electron-transfer capability of quaternized COFs are significantly enhanced in comparison to pristine COFs. These properties can be further modified through adjustments to the dimension of cyclic alkyl chain length and quaternization transformations. At 420 nm, the Tp-2C/BPy²⁺-COF containing 19.10 mol% of 2C/BPy²⁺ demonstrates the highest hydrogen evolution reaction (HER) (34 560 μ mol h⁻¹ g⁻¹, utilizing 10 mg COFs) along with a high apparent quantum efficiency (AQE) of 6.93% (Fig. 11(b) and (c)). Moreover, these exceptional results persisted throughout a 48 h photocatalytic cycle, surpassing the performance of the COF/ETM mixture system. Their approach was to maximize the utilization of 2D COFs, as a customizable platform utilized to incorporate various fundamental functions and improve photocatalytic performance synergistically via predesigned ordering frameworks.

Recently, Koyuncu and co-workers reported novel vPOPs [(TPCBP X-COF) [X = ethyl (E), butyl (B), and hexyl (H)]] where the frameworks containing a viologen moiety act as an acceptor structure and a biphenyl-bridged dicarbazole acts as an electroactive donor skeleton (Fig. 11(f)). 109 Further, TPCBP X-COF is used as a photocatalyst for the photocatalytic HER. When subjected to visible light illumination for a duration of 8 h, the H_2 evolution rate of the TPCBP B-COF (12.276 mmol g^{-1}) is 2.15 and 2.38 times greater than that of the TPCBP H-COF $(5.697 \text{ mmol h}^{-1})$ and TPCBP E-COF $(5.165 \text{ mmol h}^{-1})$, respectively (Fig. 11(g)). The TPCBP B-COF structure is regarded as one of the most effective catalysts described in the literature for photocatalytic HER; it generates 1.029 mmol g⁻¹ h⁻¹ of hydrogen and has an apparent quantum capacity of 79.69% at 470 nm (Fig. 11(h) and (i)). This approach offers fresh perspectives on the development of innovative vCOFs for the future evolution of metal-free hydrogen through solar energy conversion.

vPOPs were also considered as a remarkable heterogeneous photocatalyst for the coupling reaction but this area of research is explored very rarely. Very recently, Chen et al. reported radical cationic vPOPs (named VCR-POPs) which are intended

to facilitate metal-free photoredox catalysis of oxidative coupling of amines in the presence of visible light (Fig. 11(d)). These acetonitrile-based radical cationic vPOPs (VCR-POPs) are synthesized through a one-pot Knoevenagel condensation reaction involving 1,3,5-tris(p-formylphenyl)benzene and an acetonitrile-functionalized viologen-based ionic monomer (VIL-CN). It is noteworthy that the VCR-POPs obtained a stable viologen cationic radical, which likely underwent in situ singleelectron reduction of the dicationic monomer VIL-CN during the Knoevenagel condensation reaction facilitated by the base catalyst Cs₂CO₃. The electron paramagnetic resonance spectrum and X-ray photoelectron spectroscopy were employed to validate the radical nature of the prototypical porous organic polymer VCR-POP-1. Compared to the ionic monomer VIL-CN, the optical and electrochemical properties of VCR-POP-1 demonstrate its semiconductor nature, exceptional lightharvesting capability, and enhanced charge separation and transfer efficiency due to its well-designed cationic radical polymer structure (Fig. 11(e)). Hence, by virtue of the predominant reactive oxygen species of singlet oxygen, the polymer VCR-POP-1 featuring π-conjugated structures and viologenbased cationic radicals may be considered a metal-free heterogeneous photocatalyst that exhibits exceptional efficiency in facilitating the oxidative coupling of amines in air driven by visible light.

Outlook and summary

In this review, we have provided a comprehensive overview of the synthesis of vPOPs through several synthetic methods and their various potential applications for energy and environmental remediation. Diverse methodologies were deliberated about the synthesis of vPOPs, including solvothermal, microwave, and room temperature approaches, as well as name reactions including Zincke, Schiff base, Menshtutkin, and others. vPOPs possess excellent chemical stability with reversible redox state characteristics and have been extensively utilized in the fields such as energy storage/conversion, gas absorption/storage, toxic pollutant removal, iodine uptake and catalysis reaction. Recent years have witnessed a substantial increase in the structural diversity of vPOPs, which has also resulted in an expansion of the energy and environmental remediation applications of vPOPs. Due to their exceptional chemical stability and redox activity, vPOPs are more promising materials for employment in environmental and energy restoration.

The strategies employed for the synthesis of vPOPs are antiquated and devoid of progress in this domain. The majority of crystalline vPOPs were synthesized through the microwave method. However, solvothermal or room temperature synthetic approaches ended up with amorphous or semi-crystalline vPOPs. Surprisingly, synthesis of vPOPs at room temperature is very rare and less attempted. Room temperature synthesis offers several advantages over solvothermal synthesis or microwave synthesis. Synthesizing crystalline vPOPs at room

Materials Advances Review

temperature is a significant challenge as the reaction follows sluggish kinetics of crystallization. Therefore, researchers should explore innovative strategies, such as the use of tailored molecular precursors or novel templating agents, to overcome these barriers and develop efficient room-temperature synthesis protocols for crystalline vPOPs. Such advancements could revolutionize the field by enabling highly scalable and sustainable production of these materials for a wide range of applications.

We believe that significant studies have been achieved in energy and environmental remediation with the advent of vPOPs; however, there remain unresolved obstacles and challenges that necessitate attention. A significant obstacle is the presence of clogged surface regions on vPOPs, which arise from the occlusion of pores by counter anions. This occlusion hinders the uniform distribution of active sites with the desired porosity. To address these challenges, it is strongly encouraged that researchers prioritize template synthesis of vPOPs to achieve surface and pore size homogeneity; synthesize templateassisted thin layers; or implement 3D architectures onto vPOPs to enhance the likelihood of achieving uniform pore distribution. Limited research has been conducted on hybrid materials and vPOPs such as the implementation of macrocycle inside the vPOPs, or metal composite vPOPs, etc. Integrating viologens and other functional molecules into polymers holds significant promise and can significantly expand the range of applications for materials based on viologens. Fine-tuning mechanical properties through the selection of axle and macrocycle structures could yield valuable insights for optimizing applications, such as the utilization of resilient materials in flow experiments to remove pollutants through membranes. Presently, researchers have focused predominantly on the synthesis of vPOPs at laboratorybased small scale and showcasing their application in different directions. However, vPOPs exhibit immense potential for industrial-scale applications due to their unique combination of properties, including redox molecular switches and chemical stability. These materials offer solutions to a wide range of challenges in sectors such as gas storage, separation, catalysis, wastewater treatment, etc. In the future, transitioning vPOPs from laboratory-scale synthesis to industrial production could revolutionize various industries by providing efficient and cost-effective solutions. Scaling up production processes requires addressing challenges related to reproducibility, scalability, and costeffectiveness. However, with continued research and development efforts, along with advancements in synthesis methodologies and manufacturing techniques, vPOPs have the opportunity to make a significant impact on industrial processes, leading to sustainable and innovative solutions for energy and environmental remediation. Regarding this matter, vPOPs' structures can be strategically designed when particular applications are identified by analysing the correlations between functionality, performance, and pore structure. Notwithstanding these obstacles, the immense capacity of vPOPs as adsorbents and catalysts is substantial in terms of environmental remediation and energy conversion, and will likely inspire additional developments in structural chemistry and practical implementations. The unique coordinated sites, donoracceptor structure, and electrostatic interactions within vPOPs

make them a promising framework for resource recycling and energy conversion.

Abbreviation

EtOH Ethanol MeOH Methanol

DCM Dichloromethane

DMF N,N'-dimethylformamide

MeCN Acetonitrile THF Tetrahydrofuran Acetic acid **AcOH** BuOH Butanol

o-DCB Ortho dichlorobenzene

Conflicts of interest

There are no conflicts to declare.

Acknowledgements

PJ acknowledges VIT Vellore for the teaching and research assistant (TRA) fellowship. TP acknowledges the financial assistance of Council of Scientific & Industrial Research (CSIR, India) (sanction no: 01/3130/23 EMR-II) and SERB start-up research grant SRG/2020/001108 from the Government of India.

References

- 1 J. Zhang, Z. Zhao, Z. Xia and L. Dai, A metal-free bifunctional electrocatalyst for oxygen reduction and oxygen evolution reactions, Nat. Nanotechnol., 2015, 10, 444-452.
- 2 P. J. J. Alvarez, C. K. Chan, M. Elimelech, N. J. Halas and D. Villagrán, Emerging opportunities for nanotechnology to enhance water security, Nat. Nanotechnol., 2018, 13,
- 3 World Population Prospects: The 2015 Revision, Methodology of the United Nations Population Estimates and Projections; Working Paper No. ESA/P/WP.242; Department of Economic and Social Affairs, Population Division, United Nations, 2015.
- 4 H. A. Gasteiger and N. M. Marković, Just a Dream-or Future Reality?, Science, 2009, 324, 48-49.
- 5 D.-H. Yang, Y. Tao, X. Ding and B.-H. Han, Porous organic polymers for electrocatalysis, Chem. Soc. Rev., 2022, 51,
- 6 V. R. Stamenkovic, D. Strmcnik, P. P. Lopes and N. M. Markovic, Energy and fuels from electrochemical interfaces, Nat. Mater., 2016, 16, 57-69.
- 7 M. K. Debe, Electrocatalyst approaches and challenges for automotive fuel cells, Nature, 2012, 486, 43-51.
- 8 X. Zou and Y. Zhang, Noble metal-free hydrogen evolution catalysts for water splitting, Chem. Soc. Rev., 2015, 44(15), 5148-5180.

Review

9 D. Wu, F. Xu, B. Sun, R. Fu, H. He and K. Matyjaszewski, Design and Preparation of Porous Polymers, Chem. Rev.,

- 2012, 112, 3959-4015.
- 10 J. K. Sun and Q. Xu, Functional materials derived from open framework templates/precursors: synthesis and applications, Energy Environ. Sci., 2014, 7, 2071–2100.
- 11 A. G. Slater and A. I. Cooper, Porous materials. Functionled design of new porous materials, Science, 2015, 348, aaa8075.
- 12 S. Das, P. Heasman, T. Ben and S. Qiu, Porous Organic Materials: Strategic Design and Structure-Function Correlation, Chem. Rev., 2017, 117(3), 1515-1563.
- 13 P. Kaur, J. T. Hupp and S. T. Nguyen, Porous Organic Polymers in Catalysis: Opportunities and Challenges, ACS Catal., 2011, 1, 819-835.
- 14 H. Furukawa, K. E. Cordova, M. O'Keeffe and O. M. Yaghi, The Chemistry and Applications of Metal-Organic Frameworks, Science, 2013, 341, 1230444.
- 15 S. Kandambeth, K. Dey and R. Banerjee, Covalent Organic Frameworks: Chemistry beyond the Structure, J. Am. Chem. Soc., 2019, 141, 1807-1822.
- 16 (a) M. S. Lohse and T. Bein, Covalent Organic Frameworks: Structures, Synthesis, and Applications, Adv. Funct. Mater., 2018, 28, 1705553; (b) S. Kumar, N. M. Aldaqqa, E. Alhseinat and D. Shetty, Electrode Materials for Desalination of Water via Capacitive Deionization, Angew. Chem., Int. Ed., 2023, 62, e202302180.
- 17 K. Geng, T. He, R. Liu, S. Dalapati, K. T. Tan, Z. Li, S. Tao, Y. Gong, Q. Jiang and D. Jiang, Covalent Organic Frameworks: Design, Synthesis, and Functions, Chem. Rev., 2020, **120**, 8814-8933.
- 18 A. Trewin and A. I. Cooper, Porous organic polymers: distinction from disorder?, Angew. Chem., Int. Ed., 2010, 49, 1533-1535.
- 19 S. Fajal, S. Dutta and S. K. Ghosh, Porous organic polymers (POPs) for environmental remediation, Mater. Horiz., 2023, 10, 4083-4138.
- 20 A. Giri, Y. Khakre, G. Shreeraj, T. K. Dutta, S. Kundu and A. Patra, The order-disorder conundrum: a trade-off between crystalline and amorphous porous organic polymers for taskspecific applications, J. Mater. Chem. A, 2022, 10, 17077-17121.
- 21 J. H. Kim, D. W. Kang, H. Yun, M. Kang, N. Singh, J. S. Kim and C. S. Hong, Post-synthetic modifications in porous organic polymers for biomedical and related applications, Chem. Soc. Rev., 2022, 51, 43-56.
- 22 L. Tan and B. Tan, Hypercrosslinked porous polymer materials: design, synthesis, and applications, Chem. Soc. Rev., 2017, 46, 3322-3356.
- 23 T. Zhou, X. Huang, N. Ding, Z. Lin, Y. Yao and J. Guo, Porous polyelectrolyte frameworks: synthesis, post-ionization and advanced applications, Chem. Soc. Rev., 2022, 51, 237-267.
- 24 P. Jhariat, P. Kumari and T. Panda, Structural features of proton-conducting metal organic and covalent organic frameworks, CrystEngComm, 2020, 22, 6425-6443.
- 25 B. Zheng, X. Lin, X. Zhang, D. Wu and K. Matyjaszewski, Emerging Functional Porous Polymeric and Carbonaceous

- Materials for Environmental Treatment and Energy Storage, Adv. Funct. Mater., 2020, 30, 1907006.
- 26 S. Sarkar, T. Ghosh, A. Chakrobarty, J. Majhi, P. Nag, A. Bandyopadhyay, S. R. Vennapusa, R. Kumar and S. Mukhopadhyay, Exploring a Redox-Active Ionic Porous Organic Polymer in Environmental Remediation and Electrochromic Application, ACS Appl. Mater. Interfaces, 2023, 15, 28453-28464.
- 27 A. K. Mohammed and D. Shetty, Macroscopic covalent organic framework architectures for water remediation, Environ. Sci.: Water Res. Technol., 2021, 7, 1895-1927.
- 28 W. Xie, D. Cui, S.-R. Zhang, Y.-H. Xu and D.-L. Jiang, Iodine capture in porous organic polymers and metal-organic frameworks materials, Mater. Horiz., 2019, 6, 1571-1595.
- 29 Z. Wang, S. Zhang, Y. Chen, Z. Zhang and S. Ma, Covalent organic frameworks for separation applications, Chem. Soc. Rev., 2020, 49, 708-735.
- 30 J. Winsberg, T. Hagemann, T. Janoschka, M. D. Hager and U. S. Schubert, Redox-Flow Batteries: From Metals to Organic Redox-Active Materials, Angew. Chem., Int. Ed., 2017, 56, 686-711.
- 31 K. Madasamy, D. Velayutham, V. Suryanarayanan, M. Kathiresan and K.-C. Ho, Viologen-based electrochromic materials and devices, J. Mater. Chem. C, 2019, 7, 4622-4637.
- 32 J. Ding, C. Zheng, L. Wang, C. Lu, B. Zhang, Y. Chen, M. Li, G. Zhai and X. Zhuang, Viologen-inspired functional materials: synthetic strategies and applications, J. Mater. Chem. A, 2019, 7, 23337-23360.
- 33 (a) T. Skorjanc, D. Shetty, M. A. Olson and A. Trabolsi, Design Strategies and Redox-Dependent Applications of Insoluble Viologen-Based Covalent Organic Polymers, ACS Appl. Mater. Interfaces, 2019, 11, 6705-6716; (b) G. Chen, Y. Zhou, X. Wang, J. Li, S. Xue, Y. Liu, Q. Wang and J. Wang, Construction of porous cationic frameworks by crosslinking polyhedral oligomeric silsesquioxane units with N-heterocyclic linkers, Sci. Rep., 2015, 5, 11236.
- 34 L. Striepe and T. Baumgartner, Viologens and Their Application as Functional Materials, Chem. - Eur. J., 2017, 23, 16924-16940.
- 35 K. Madasamy and M. Kathiresan, Dimeric and Star-Shaped Viologens: Synthesis and Capping interactions with βcyclodextrin, ChemistrySelect, 2016, 1, 354-359.
- 36 K. Murugavel, Benzylic viologen dendrimers: a review of their synthesis, properties and applications, Polym. Chem., 2014, 5, 5873-5884.
- 37 M. Burgess, E. Chénard, K. Hernández-Burgos, G. Nagarjuna, R. S. Assary, J. Hui, J. S. Moore and J. Rodríguez-López, Impact of Backbone Tether Length and Structure on the Electrochemical Performance of Viologen Redox Active Polymers, Chem. Mater., 2016, 28, 7362-7374.
- 38 M. J. Juetten, A. T. Buck and A. H. Winter, A radical spin on viologen polymers: organic spin crossover materials in water, Chem. Commun., 2015, 51, 5516-5519.
- 39 C. L. Bird and A. T. Kuhn, Electrochemistry of the viologens, Chem. Soc. Rev., 1981, 10, 49-82.

40 M. R. Geraskina, A. S. Dutton, M. J. Juetten, S. A. Wood and A. H. Winter, The Viologen Cation Radical Pimer A Case of Dispersion-Driven Bonding, Angew. Chem., Int. Ed., 2017, 56, 9435-9439.

Materials Advances

- 41 C. Monterde, R. Navarro, M. Iglesias and F. Sánchez, Fluorine-Phenanthroimidazole Porous Organic Polymer Efficient Microwave Synthesis and Photocatalytic Activity, ACS Appl. Mater. Interfaces, 2019, 11, 3459-3465.
- 42 Z. Zhang, J. Jia, Y. Zhi, S. Ma and X. Liu, Porous organic polymers for light-driven organic transformations, Chem. Soc. Rev., 2022, 51, 2444-2490.
- 43 G. Das, T. Skorjanc, S. K. Sharma, F. Gándara, M. Lusi, D. S. Shankar Rao, S. Vimala, S. Krishna Prasad, J. Raya, D. S. Han, R. Jagannathan, J.-C. Olsen and A. Trabolsi, Viologen-Based Conjugated Covalent Organic Networks via Zincke Reaction, J. Am. Chem. Soc., 2017, 139, 9558-9565.
- 44 T. Skorjanc, D. Shetty, F. Gándara, S. Pascal, N. Naleem, S. Abubakar, L. Ali, A. K. Mohammed, J. Raya, S. Kirmizialtin, O. Siri and A. Trabolsi, Covalent Organic Framework Based on Azacalix[4]arene for the Efficient Capture of Dialysis Waste Products, ACS Appl. Mater. Interfaces, 2022, 14, 39293-39298.
- 45 L.-Z. Peng, P. Liu, Q.-Q. Cheng, W.-J. Hu, Y. A. Liu, J.-S. Li, B. Jiang, X.-S. Jia, H. Yang and K. Wen, Highly effective electrosynthesis of hydrogen peroxide from oxygen on a redox-active cationic covalent triazine network, Chem. Commun., 2018, 54, 4433-4436.
- 46 P. Samanta, P. Chandra, S. Dutta, A. V. Desai and S. K. Ghosh, Chemically stable ionic viologen-organic network an efficient scavenger of toxic oxo-anions from water, Chem. Sci., 2018, 9, 7874-7881.
- 47 Z. Wang, X. Jia, P. Zhang, Y. Liu, H. Qi, P. Zhang, U. Kaiser, S. Reineke, R. Dong and X. Feng, Viologen-Immobilized 2D Polymer Film Enabling Highly Efficient Electrochromic Device for Solar-Powered Smart Window, Adv. Mater., 2022, 34, 2106073.
- 48 G. Das, S. K. Sharma, T. Prakasam, F. Gándara, R. Mathew, N. Alkhatib, N. I. Saleh, R. Pasricha, J.-C. Olsen, M. Baias, S. Kirmizialtin, R. Jagannathan and A. Trabolsi, A polyrotaxanated covalent organic network based on viologen and cucurbit[7]uril, Commun. Chem., 2019, 2, 106.
- 49 F. Ahmadijokani, A. Ghaffarkhah, H. Molavi, S. Dutta, Y. Lu, S. Wuttke, M. Kamkar, O. J. Rojas and M. Arjmand, COF and MOF Hybrids Advanced Materials for Wastewater Treatment, Adv. Funct. Mater., 2023, 2305527.
- 50 Z. Xia, Y. Zhao and S. B. Darling, Covalent Organic Frameworks for Water Treatment, Adv. Mater. Interfaces, 2021, 8, 2001507.
- 51 Y. Mou, X. Yuan, H. Chen, Y. Yang, H. Dai, J. Bai, J. Chen, J. W. Chew, H. Wang and Y. Wu, Reticular materials for wastewater treatment, J. Mater. Chem. A, 2023, 11, 22631-22655.
- 52 S. Bolisetty, M. Peydayesh and R. Mezzenga, Sustainable technologies for water purification from heavy metals review and analysis, Chem. Soc. Rev., 2019, 48, 463-487.
- 53 J. R. Werber, C. O. Osuji and M. Elimelech, Materials for next-generation desalination and water purification membranes, Nat. Rev. Mater., 2016, 1, 1-15.

- 54 I. Ali, New Generation Adsorbents for Water Treatment, Chem. Rev., 2012, 112, 5073-5091.
- 55 S. Roy Barman, P. Gavit, S. Chowdhury, K. Chatterjee and A. Nain, 3D-Printed Materials for Wastewater Treatment, IACS Au, 2023, 3, 2930-2947.
- 56 S. Rojas and P. Horcajada, Metal-Organic Frameworks for the Removal of Emerging Organic Contaminants in Water, Chem. Rev., 2020, 120, 8378-8415.
- 57 Y. Zhang, X. Hong, X.-M. Cao, X.-Q. Huang, B. Hu, S.-Y. Ding and H. Lin, Functional Porous Organic Polymers with Conjugated Triaryl Triazine as the Core for Superfast Adsorption Removal of Organic Dyes, ACS Appl. Mater. Interfaces, 2021, 13, 6359-6366.
- 58 S. Fajal, A. Hassan, W. Mandal, M. M. Shirolkar, S. Let, N. Das and S. K. Ghosh, Ordered Macro/Microporous Ionic Organic Framework for Efficient Separation of Toxic Pollutants from Water, Angew. Chem., Int. Ed., 2023, 62, e202214095.
- 59 G. Das, T. Skorjanc, T. Prakasam, S. Nuryyeva, J.-C. Olsen and A. Trabolsi, Microwave-assisted synthesis of a viologen-based covalent organic polymer with redoxtunable polarity for dye adsorption, RSC Adv., 2017, 7, 3594-3598.
- 60 S.-B. Yu, H. Lyu, J. Tian, H. Wang, D.-W. Zhang, Y. Liu and Z.-T. Li, A polycationic covalent organic framework a robust adsorbent for anionic dye pollutants, Polym. Chem., 2016, 7, 3392-3397.
- 61 B. Li, Y. Zhang, D. Ma, Z. Xing, T. Ma, Z. Shi, X. Ji and S. Ma, Creation of a new type of ion exchange material for rapid, high-capacity, reversible and selective ion exchange without swelling and entrainment, Chem. Sci., 2016, 7, 2138-2144.
- 62 Q. Sun, B. Aguila, Y. Song and S. Ma, Tailored Porous Organic Polymers for Task-Specific Water Purification, Acc. Chem. Res., 2020, 53(4), 812-821.
- 63 S. Dutta, S. Let, S. Sharma, D. Mahato and S. K. Ghosh, Recognition and Sequestration of Toxic Inorganic Water Pollutants with Hydrolytically Stable Metal-Organic Frameworks, Chem. Rec., 2021, 21, 1666-1680.
- 64 P. Samanta, A. V. Desai, S. Let and S. K. Ghosh, Advanced Porous Materials for Sensing, Capture and Detoxification of Organic Pollutants toward Water Remediation, ACS Sustainable Chem. Eng., 2019, 7, 7456-7478.
- 65 M. Ding, L. Chen, Y. Xu, B. Chen, J. Ding, R. Wu, C. Huang, Y. He, Y. Jin and C. Xia, Efficient capture of Tc/Re(vii, iv) by a viologen-based organic polymer containing tetraaza macrocycles, J. Chem. Eng., 2020, 380, 122581.
- 66 Y. Huang, M. Ding, J. Ding, J. Kang, Z. Yan, P. Zhao, X. Zhou, Y. Jin, S. Chen and C. Xia, Targeted synthesis of a high-stability cationic porous aromatic framework for highly efficient remediation of 99TcO₄-, J. Chem. Eng., 2022, 435, 134785.
- 67 X.-R. Chen, C.-R. Zhang, W. Jiang, X. Liu, Q.-X. Luo, L. Zhang, R.-P. Liang and J.-D. Qiu, 3D Viologen-based covalent organic framework for selective and efficient adsorption of ReO₄⁻/TcO₄⁻, Sep. Purif. Technol., 2023, 312, 123409.

Review

68 Z. Yan, Y. Yuan, Y. Tian, D. Zhang and G. Zhu, Highly Efficient Enrichment of Volatile Iodine by Charged Porous Aromatic Frameworks with Three Sorption Sites, Angew. Chem., Int. Ed., 2015, 54, 12733-12737.

- 69 T. Skorjanc, D. Shetty, S. K. Sharma, J. Raya, H. Traboulsi, D. S. Han, J. Lalla, R. Newlon, R. Jagannathan, S. Kirmizialtin, J.-C. Olsen and A. Trabolsi, Redox-Responsive Covalent Organic Nanosheets from Viologens and Calix[4]arene for Iodine and Toxic Dye Capture, Chem. - Eur. J., 2018, 24, 8648-8655.
- 70 G. Das, T. Prakasam, S. Nuryyeva, D. S. Han, A. Abdel-Wahab, J.-C. Olsen, K. Polychronopoulou, C. Platas-Iglesias, F. Ravaux, M. Jouiad and A. Trabolsi, Multifunctional redox-tuned viologen-based covalent organic polymers, J. Mater. Chem. A, 2016, 4, 15361-15369.
- 71 G. Férey, C. Serre, T. Devic, G. Maurin, H. Jobic, P. L. Llewellyn, G. De Weireld, A. Vimont, M. Daturi and J.-S. Chang, Why hybrid porous solids capture greenhouse gases?, Chem. Soc. Rev., 2011, 40, 550-562.
- 72 K. S. Song, P. W. Fritz and A. Coskun, Porous organic polymers for CO₂ capture, separation and conversion, Chem. Soc. Rev., 2022, 51, 9831-9852.
- 73 H. A. Patel, S. Hyun Je, J. Park, D. P. Chen, Y. Jung, C. T. Yavuz and A. Coskun, Unprecedented hightemperature CO₂ selectivity in N₂-phobic nanoporous covalent organic polymers, Nat. Commun., 2013, 4, 1357.
- 74 O. Buyukcakir, S. H. Je, D. S. Choi, S. N. Talapaneni, Y. Seo, Y. Jung, K. Polychronopoulou and A. Coskun, Porous cationic polymers the impact of counteranions and charges on CO₂ capture and conversion, Chem. Commun., 2016, 52, 934-937.
- 75 O. Buyukcakir, S. H. Je, S. N. Talapaneni, D. Kim and A. Coskun, Charged Covalent Triazine Frameworks for CO2 Capture and Conversion, ACS Appl. Mater. Interfaces, 2017, 9, 7209-7216.
- 76 C. Hua, B. Chan, A. Rawal, F. Tuna, D. Collison, J. M. Hook and D. M. D'Alessandro, Redox tunable viologen-based porous organic polymers, J. Mater. Chem. C, 2016, 4, 2535-2544.
- 77 Y. Zhang, K. Liu, L. Wu, H. Zhong, N. Luo, Y. Zhu, M. Tong, Z. Long and G. Chen, Silanol-Enriched Viologen-Based Ionic Porous Hybrid Polymers for Efficient Catalytic CO2 Fixation into Cyclic Carbonates under Mild Conditions, ACS Sustainable Chem. Eng., 2019, 7, 16907-16916.
- 78 G. Chen, X. Huang, Y. Zhang, M. Sun, J. Shen, R. Huang, M. Tong, Z. Long and X. Wang, Constructing POSS and viologen-linked porous cationic frameworks induced by the Zincke reaction for efficient CO2 capture and conversion, Chem. Commun., 2018, 54, 12174-12177.
- 79 M. Kathiresan, B. Ambrose, N. Angulakshmi, D. E. Mathew, D. Sujatha and A. M. Stephan, Viologens a versatile organic molecule for energy storage applications, J. Mater. Chem. A, 2021, 9, 27215-27233.
- 80 P. Jhariat, A. Warrier, A. Sasmal, S. Das, S. Sarfudeen, P. Kumari, A. K. Nayak and T. Panda, Reticular synthesis of two-dimensional ionic covalent organic networks as metal-free bifunctional electrocatalysts for oxygen

- reduction and evolution reactions, Nanoscale, 2024, 16, 5665-5673.
- 81 Z. Wang, Q. Qi, W. Jin, X. Zhao, X. Huang and Y. Li, Trapping Halogen Anions in Cationic Viologen Porous Organic Polymers for Highly Cycling-Stable Cathode Materials, Small, 2023, 19, 2303430.
- 82 T. Skorjanc, D. Shetty, F. Gándara, L. Ali, J. Raya, G. Das, M. A. Olson and A. Trabolsi, Remarkably efficient removal of toxic bromate from drinking water with a porphyrin-viologen covalent organic framework, Chem. Sci., 2020, 11, 845-850.
- 83 D. Chakraborty, S. Nandi, R. Kushwaha, D. Kaleeswaran and R. Vaidhyanathan, Viologen functionalized C-C bonded cationic polymers for oxo-anion pollutant removal from aqueous medium, Mater. Res. Bull., 2022, 146, 111614.
- 84 X. Zhang, Y.-Z. Yuan, H.-F. Li, Q.-J. Wu, H.-J. Zhu, Y.-L. Dong, Q. Wu, Y.-B. Huang and R. Cao, Viologen linker as a strong electron-transfer mediator in the covalent organic framework to enhance electrocatalytic CO₂ reduction, Mater. Chem. Front., 2023, 7, 2661-2670.
- 85 L. Liu, W.-D. Qu, K.-X. Dong, Y. Qi, W.-T. Gong, G.-L. Ning and J.-N. Cui, An anthracene extended viologenincorporated ionic porous organic polymer for efficient aerobic photocatalysis and antibacterial activity, Chem. Commun., 2021, 57, 3339-3342.
- 86 L. He, S. Liu, L. Chen, X. Dai, J. Li, M. Zhang, F. Ma, C. Zhang, Z. Yang, R. Zhou, Z. Chai and S. Wang, Mechanism unravelling for ultrafast and selective 99TcO4 uptake by a radiation-resistant cationic covalent organic framework a combined radiological experiment and molecular dynamics simulation study, Chem. Sci., 2019, 10, 4293-4305.
- 87 H.-Z. Li, C. Yang, H.-L. Qian and X.-P. Yan, Roomtemperature synthesis of ionic covalent organic frameworks for efficient removal of diclofenac sodium from aqueous solution, Sep. Purif. Technol., 2023, 306, 122704.
- 88 Y. Zhang, K. Zhang, L. Wu, K. Liu, R. Huang, Z. Long, M. Tong and G. Chen, Facile synthesis of crystalline viologen-based porous ionic polymers with hydrogenbonded water for efficient catalytic CO2 fixation under ambient conditions, RSC Adv., 2020, 10, 3606-3614.
- 89 G. Das, T. Skorjanc, S. K. Sharma, T. Prakasam, C. Platas-Iglesias, D. S. Han, J. Raya, J.-C. Olsen, R. Jagannathan and A. Trabolsi, Morphological Diversity in Nanoporous Covalent Organic Materials Derived from Viologen and Pyrene, ChemNanoMat, 2018, 4, 61-65.
- 90 X. Shen, S. Ma, H. Xia, Z. Shi, Y. Mu and X. Liu, Cationic porous organic polymers as an excellent platform for highly efficient removal of pollutants from water, J. Mater. Chem. A, 2018, 6, 20653-20658.
- 91 A. Hassan, M. M. R. Mollah, S. Das and N. Das, Rapid and selective removal of toxic and radioactive anionic pollutants using an ionic covalent organic framework (iCOF-2), J. Mater. Chem. A, 2023, 11, 17226-17236.
- 92 S. Jiao, L. Deng, X. Zhang, Y. Zhang, K. Liu, S. Li, L. Wang and D. Ma, Evaluation of an Ionic Porous Organic Polymer for Water Remediation, ACS Appl. Mater. Interfaces, 2021, 13, 39404-39413.

93 Z.-J. Li, H.-D. Xue, Y.-Q. Zhang, H.-S. Hu and X.-D. Zheng, Construction of a cationic organic network for highly efficient removal of anionic contaminants from water, New J. Chem., 2019, 43, 11604-11609.

Materials Advances

94 X. Li, M. Zhou, J. Jia and O. Jia, A water-insoluble viologenbased β-cyclodextrin polymer for selective adsorption toward anionic dyes, React. Funct. Polym., 2018, 126, 20-26.

- 95 (a) S. T. Kostakoğlu, Y. Chumakov, Y. Zorlu, A. E. Sadak, S. Denizaltı, A. G. Gürek and M. M. Ayhan, Elucidating the role of non-covalent interactions in unexpectedly high and selective CO2 uptake and catalytic conversion of porphyrinbased ionic organic polymers, Mater. Adv., 2021, 2, 3685-3694; (b) Z. Xu, K. Liu, H. Huang, Y. Zhang, Z. Long, M. Tong and G. Chen, Quaternization-induced catalyst-free synthesis of viologen-linked ionic polyacetylenes towards heterogeneous catalytic CO₂ fixation, *J. Mater. Chem.* A, 2022, 10, 5540-5549.
- 96 Y. Chen, R. Luo, Q. Xu, J. Jiang, X. Zhou and H. Ji, Metalloporphyrin Polymers with Intercalated Ionic Liquids for Synergistic CO2 Fixation via Cyclic Carbonate Production, ACS Sustainable Chem. Eng., 2018, 6, 1074-1082.
- 97 J. Chakraborty, I. Nath and F. Verpoort, A physicochemical introspection of porous organic polymer photocatalysts for wastewater treatment, Chem. Soc. Rev., 2022, 51, 1124-1138.
- 98 T. Zhang, V. G. Gregoriou, N. Gasparini and C. L. Chochos, Porous organic polymers in solar cells, Chem. Soc. Rev., 2022, 51, 4465-4483.
- 99 Y. Zhang and S. N. Riduan, Functional porous organic polymers for heterogeneous catalysis, Chem. Soc. Rev., 2012, 41, 2083-2094.
- 100 T. Endo, K. Ageishi and M. Okawara, Reduction of acrylonitrile in the presence of viologen derivatives, J. Org. Chem., 1986, 51, 4309-4310.
- 101 J.-K. Tang, S.-B. Yu, C.-Z. Liu, H. Wang, D.-W. Zhang and Z.-T. Li, A Highly Stable Porous Viologen Polymer for the Catalysis of Debromination Coupling of Benzyl Bromides with High Recyclability, Asian J. Org. Chem., 2019, 8, 1912-1918.

- 102 C. Yadav, S. Payra and J. N. Moorthy, Ionic porous organic polymer (IPOP) based on twisted biphenyl Scaffold Green and efficient heterogeneous catalytic synthesis of β -Arylthioketones and biscoumarins, J. Catal., 2022, 413, 769-778.
- 103 H. Luo, S. Wang, X. Meng, G. Yuan, X. Song and Z. Liang, A hollow viologen-based porous organic polymer for the catalytic cycloaddition of CO₂, Mater. Chem. Front., 2023, 7, 2277-2285.
- 104 Y. Zhang, T. Mori, J. Ye and M. Antonietti, Phosphorus-Doped Carbon Nitride Solid Enhanced Electrical Conductivity and Photocurrent Generation, J. Am. Chem. Soc., 2010, 132, 6294-6295.
- 105 J. Byun and K. A. I. Zhang, Designing conjugated porous polymers for visible light-driven photocatalytic chemical transformations, Mater. Horiz., 2020, 7, 15-31.
- 106 Z. Mi, P. Yang, R. Wang, J. Unruangsri, W. Yang, C. Wang and J. Guo, Stable Radical Cation-Containing Covalent Organic Frameworks Exhibiting Remarkable Structure-Enhanced Photothermal Conversion, I. Am. Chem. Soc., 2019, 141, 14433-14442.
- 107 Z. Mi, T. Zhou, W. Weng, J. Unruangsri, K. Hu, W. Yang, C. Wang, K. A. I. Zhang and J. Guo, Covalent Organic Frameworks Enabling Site Isolation of Viologen-Derived Electron-Transfer Mediators for Stable Photocatalytic Hydrogen Evolution, Angew. Chem., Int. Ed., 2021, 60, 9642-9649.
- 108 M. Isegawa, Metal- and ligand-substitution-induced changes in the kinetics and thermodynamics of hydrogen activation and hydricity in a dinuclear metal complex, Dalton Trans., 2024, 53, 5966-5978.
- 109 S. Altınışık, G. Yanalak, İ. Hatay Patır and S. Koyuncu, Viologen-Based Covalent Organic Frameworks toward Metal-Free Highly Efficient Photocatalytic Hydrogen Evolution, ACS Appl. Mater. Interfaces, 2023, 15, 18836-18844.
- 110 Z. Xu, K. Liu, S. Wang, Y. Chang, J. Chen, S. Wang, C. Meng, Z. Long, Z. Qin and G. Chen, Viologen-Based Cationic Radical Porous Organic Polymers for Visible-Light-Driven Photocatalytic Oxidation, ACS Appl. Polym. Mater., 2024, 6, 701-711.